

Article

Petrography and Lithofacies of the Siwalik Group in the Core of Hazara-Kashmir Syntaxis: Implications for Middle Stage Himalayan Orogeny and Paleoclimatic Conditions

Muhammad Zaheer ^{1,*}, Muhammad Rustam Khan ¹, Muhammad Saleem Mughal ¹, Hammad Tariq Janjuhah ^{2,*} , Panayota Makri ³ and George Kontakiotis ³ 

¹ Institute of Geology, University of Azad Jammu and Kashmir, Muzaffarabad 13100, Pakistan

² Department of Geology, Shaheed Benazir Bhutto University Sheringal, Sheringal 18000, Pakistan

³ Department of Historical Geology-Paleontology, Faculty of Geology and Geoenvironment, School of Earth Sciences, National and Kapodistrian University of Athens, Panepistimiopolis, 15784 Athens, Greece

* Correspondence: zaheer.awan185@gmail.com (M.Z.); hammad@sbbu.edu.pk (H.T.J.)

Abstract: The present field and petrographic investigations of the Tortonian to Gelasian Siwalik Group in the core of the Hazara-Kashmir Syntaxis have been carried out to comprehend the middle stage Himalayan orogeny that resulted from the collision of Indian and Asian plates. The Chinji, Nagri, Dhok Pathan, and Soan Formations of the Siwalik Group were deposited by river meandering flood plains, braided rivers, and alluvial fan systems, respectively. The Siwalik Group is classified into seven major facies and many minor facies based on sedimentological properties. According to the petrographic analysis, the Siwalik Group sandstone is classified as litharenite and feldspathic litharenite petrofacies. The sandstone of the Siwalik Group is texturally mature, but compositionally it is immature. The data shown on the tectonic discrimination diagrams point to a recycled orogen provenance field for the Siwalik sandstone. In addition to quartz and feldspar, the sandstone includes clasts of volcanic, metamorphic, and sedimentary rock types. The igneous and metamorphic rock clasts were derived from the Lesser and Higher Himalayas. The sedimentary lithic fragments, on the other hand, are derived from both the earlier molasse and pre-molasse rocks. The presence of lithic fragments of the earlier molasse sandstone in the Siwalik sandstone indicates that the Siwalik Group sandstones were deposited during the Middle Stage of the Himalayan orogeny. The paleoclimatic conditions were semi-arid to semi-humid during the Siwalik Group's deposition. The presence of clay minerals in the shale reveals the intense chemical weathering processes that occurred during their deposition on the flood plains of the river meandering system.



Citation: Zaheer, M.; Khan, M.R.; Mughal, M.S.; Janjuhah, H.T.; Makri, P.; Kontakiotis, G. Petrography and Lithofacies of the Siwalik Group in the Core of Hazara-Kashmir Syntaxis: Implications for Middle Stage Himalayan Orogeny and Paleoclimatic Conditions. *Minerals* **2022**, *12*, 1055. <https://doi.org/10.3390/min12081055>

Academic Editor: Harald G. Dill

Received: 27 July 2022

Accepted: 19 August 2022

Published: 21 August 2022

Publisher's Note: MDPI stays neutral with regard to jurisdictional claims in published maps and institutional affiliations.



Copyright: © 2022 by the authors. Licensee MDPI, Basel, Switzerland. This article is an open access article distributed under the terms and conditions of the Creative Commons Attribution (CC BY) license (<https://creativecommons.org/licenses/by/4.0/>).

Keywords: Siwalik sandstones; petrography and provenance; middle stage Himalayan orogeny; depositional environment; paleoclimatic conditions; sedimentary structures; Paleoenvironmental reconstruction

1. Introduction

The Himalayas are the world's youngest, longest, and highest mountain belts, developed during the Cenozoic by the Indian plate ongoing collision with the Asian plate [1–4]. The Himalayas are categorized into four subdivisions, e.g., Sub-Himalaya, Lesser Himalaya, Higher Himalaya, and Trans-Himalaya [4,5]. The study area lies in the Sub-Himalayan region of the Potwar Plateau of Pakistan (Figures 1 and 2). The Sub-Himalayan regions, also termed as the Himalayan Foreland Basin (HFB), consist of Paleogene–Neogene sediments [6]. The Paleogene deposits of the basin are exposed only along a few sectors of the HFB and have different names in different areas. However, the Neogene alluvial strata are well exposed continuously throughout the length of the HFB, from the Indus Valley (Pakistan) in the west to the Irrawaddy Valley (Myanmar) in the east, and these deposits are known as the Siwalik Group [7].

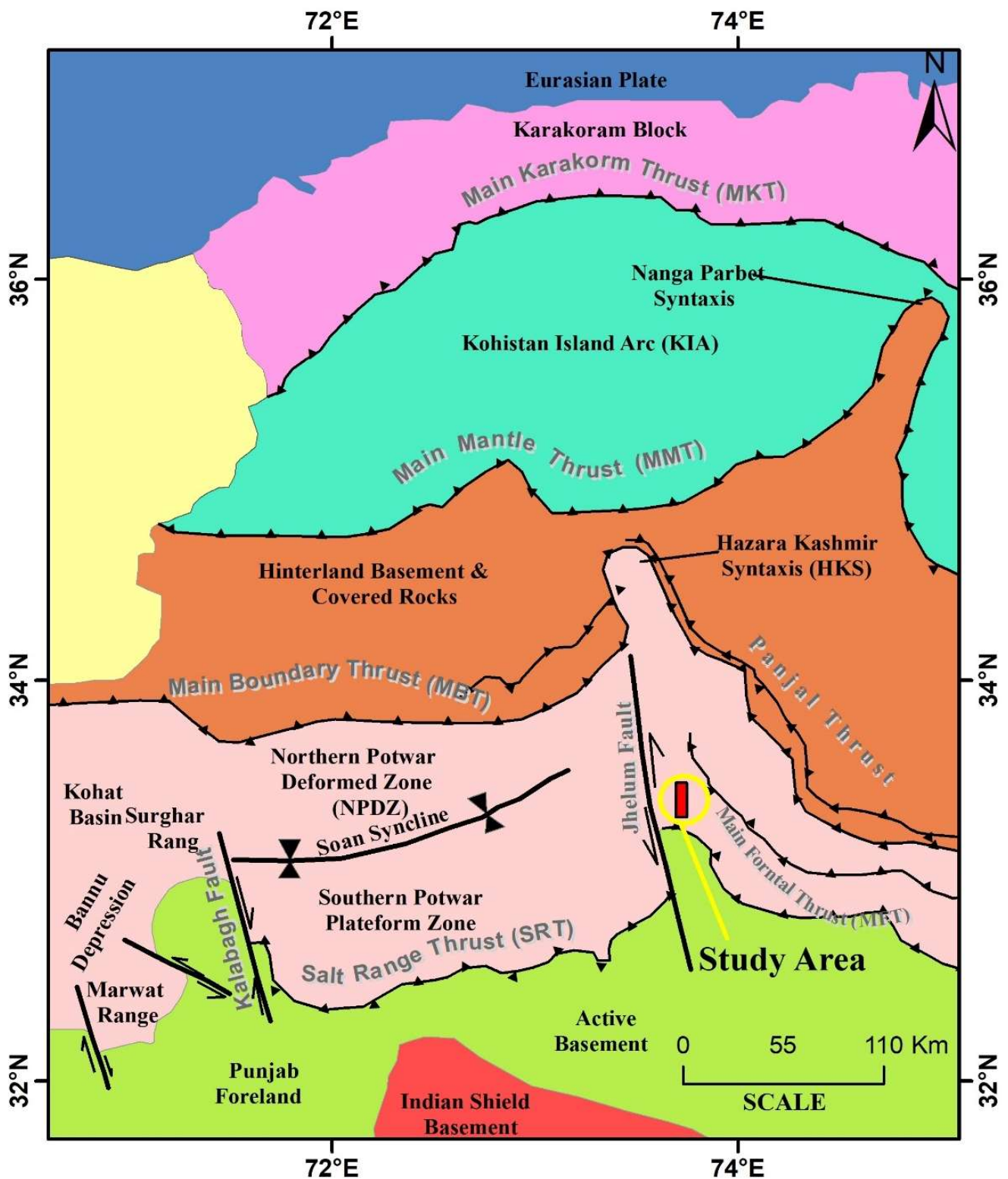


Figure 1. A northern Pakistan tectonic map showing study area (Modified and compared after Basharat, et al. [8], Avouac, et al. [9], Greco [10], Baig and Lawrence [11], Calkins, et al. [12] and Wadia [13]).

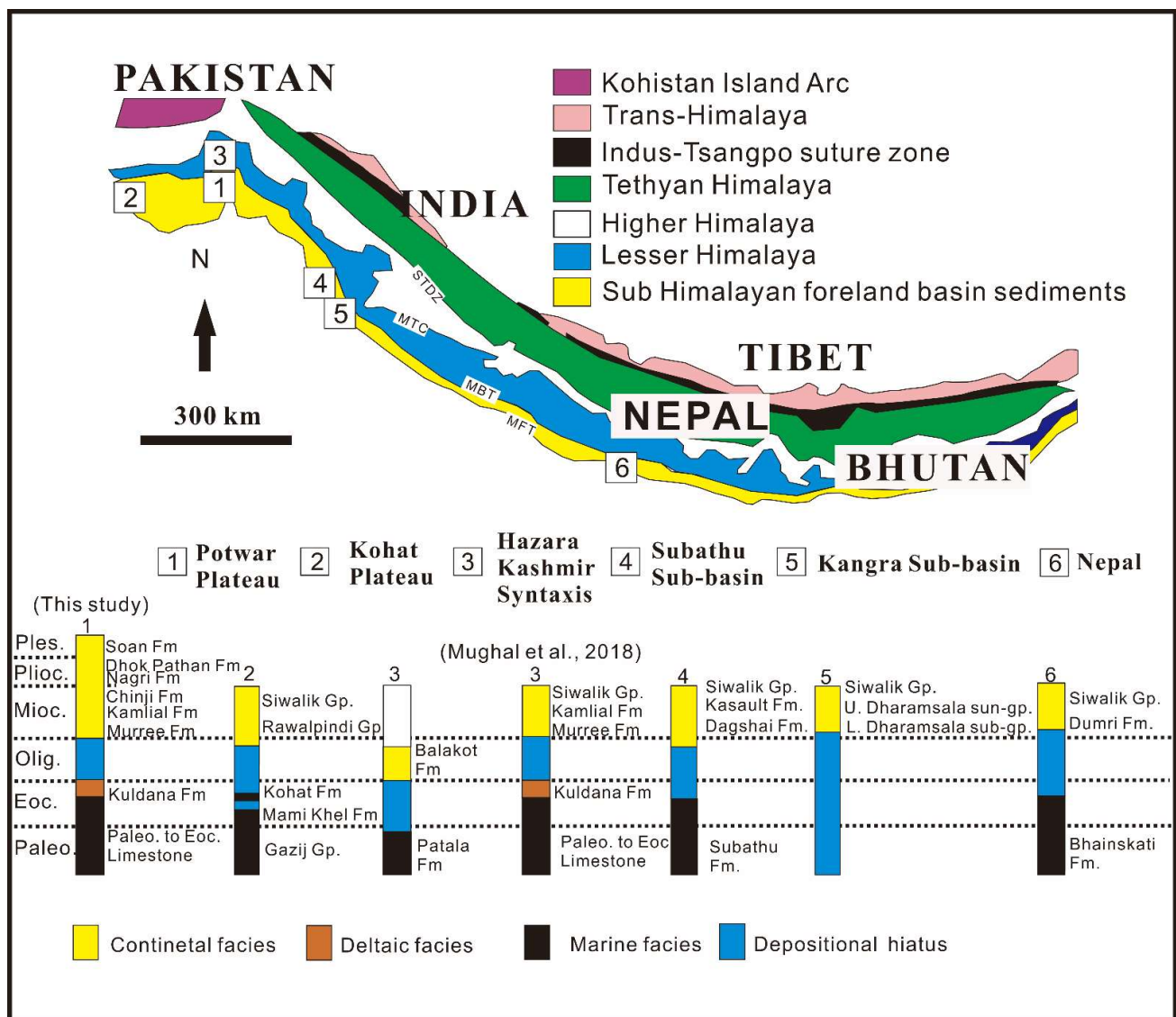


Figure 2. Simplified geological map of the Himalayan region; boxed numbers refer to stratigraphic sections in the foreland basin, modified after Mughal, Zhang, Du, Zhang, Mustafa, Hameed, Khan, Zaheer and Blaise [2]. STDZ = South Tibetan Detachment Zone, MCT = Main Central Thrust, MBT = Main Boundary Thrust, MFT = Main Frontal Thrust.

Geographically, the Siwalik Group has been widely spread into four countries, e.g., Pakistan, India, Nepal, and Bhutan (Figure 2). In the present study, the observations are confined to the Siwalik Group (Figure 3). The Siwalik Group is mainly composed of sandstone, shale, clays, and conglomerates. In Pakistan, its lower contact is conformable with the Rawalpindi Group (e.g., Muree Formation and Kamliyal Formation), whereas its upper contact with the Lei Conglomerate/Mirpur Conglomerate is unconformable. Different researchers have worked on Himalayan molasses deposits in different parts of Azad Jammu and Kashmir, Pakistan, including Najman, Garzanti, Pringle, Bickle, Stix and Khan [1], Ashraf and Chaudhary [14], Bossart, et al. [15], Critelli and Garzanti [16], Javed, et al. [17], Iqbal, et al. [18], Abbasi and Khan [19], Zaheer, et al. [20], Abbasi [21], Zaleha [22], Mustafa, et al. [23], Aadil [24], and Khan, et al. [25]. Apart from these, various other researchers have also worked on the Siwalik Group rocks of other parts of the Sub-Himalayas in India and Nepal, including Singh [26], Ghosh and Kumar [27], Sanyal, et al. [28], Kundu, et al. [29], Goswami and Deopa [7], Debnath, et al. [30], Sigdel and Sakai [31], Syangbo and Tamrakar [32], and Rai, et al. [33].

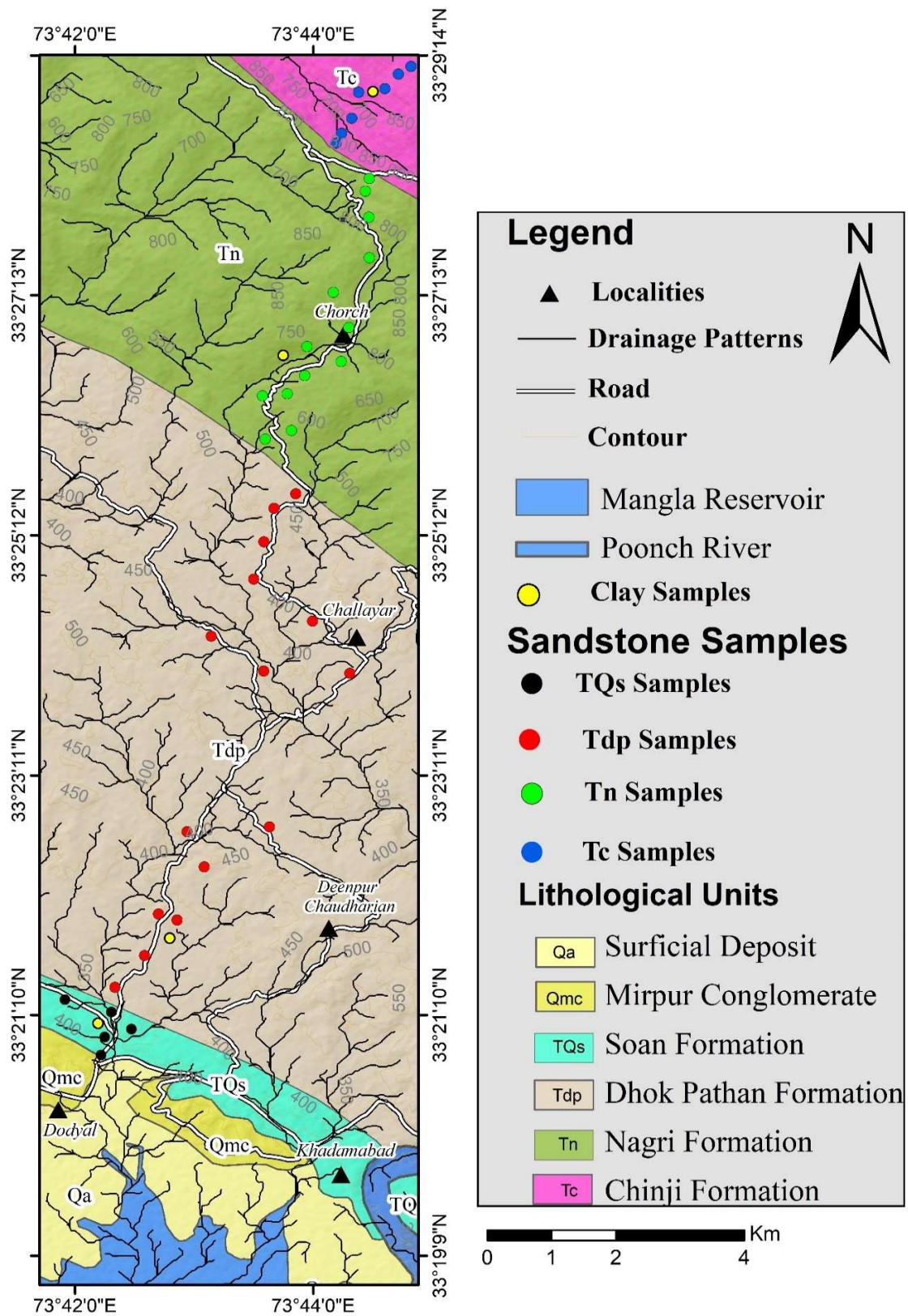


Figure 3. Geological and sample location map of the Siwalik Group in the core of HKS (Dadyal to Sehnsa section).

Khan [34] inferred that the Siwaliks of different areas had been derived from diverse source regions. The Siwalik sediments in Pakistan’s Shinghar Range are derived from the

Kohistan Island Arc, the Western Karakoram, Afghanistan, and Parachinar. Chaudhry and Ashraf [35] proved that the provenance of the Middle Siwalik rocks (Kotli, Azad Kashmir, Pakistan) derived from igneous, metamorphic, and sedimentary terrains that are located on the northeastern and northern sides of the area. According to Ullah, et al. [36] the Kamlial Formation of the Rawalpindi Group in the Kohat Plateau has been derived by the weathering of feldspar-rich crystalline rocks. Ullah, et al. [37] discussed the depositional environments and concluded that the Chinji Formation was deposited as a floodplain, whereas the Nagri Formation was deposited by a sandy bedload braided fluvial system. Ghosh and Kumar [27] inferred that the provenance of the Middle Siwalik sandstone of the Garhwal Himalaya is derived from igneous, sedimentary, and low- to medium-grade metamorphic rocks. According to Kundu, Matin, and Mukul [29] the sedimentary facies associations within the lithostratigraphic column of the Middle Siwalik rocks in the Eastern Himalaya, India (Tista Valley, Darjiling District) suggest that an oscillation occurred between proximal-, mid-, and distal fan settings within a palaeo-alluvial fan depositional environment. Goswami and Deopa [7] described the Lower Siwalik molasses of southeastern Kumaun Himalaya as comprising lithic arenites, sublithic arenites, and lithic greywacke sandstone and belonging to the quartzolitic petrofacies. Sigdel and Sakai [31] concluded that the detrital modes of the sandstones of the Siwalik Group along the Karnali River, Nepal Himalaya, indicate a recycled orogen provenance field for their deposition. Syangbo and Tamrakar [32] suggested that the depositional environment of lower Siwalik rocks in the Samari-Sukaura area of Nepal is a result of a mixed load meandering river system.

The previous researchers suggested a continental fluvial environment or marine inputs for the Siwalik Group [7,30,31,34–36,38]. They conducted reconnaissance studies on the individual formations or parts of the Siwalik Group (e.g., the lower and middle Siwaliks), and mostly they addressed only one or two aspects [7,27–35,37]. The different researchers suggested different provenances, and depositional environments for the Siwaliks. No consensus has yet been developed on the provenance, tectonic setting, paleoclimatic conditions, and depositional environment of the Siwalik Group. Furthermore, based on the petrographic investigation, the paleoclimatic conditions of the Siwalik Group have not been adequately addressed yet. Therefore, the present study is focused on the Lower–Upper Siwaliks (e.g., the Chinji, Nagri, Dhok Pathan, and Soan Formations) with different aspects in detail. A detailed field study, petrographic investigation and X-Ray Diffraction (XRD) analysis have been carried out to precisely determine the provenance, tectonic and depositional settings, and paleoclimatic conditions of the Siwalik Group.

2. Geological Setting

The study area lies in the Dadyal to Sehnsa region of Mirpur, a division of Azad Kashmir, Pakistan, and is bounded by latitude and longitude, which range from 33°20′08″ to 33°29′14″ N and 73°41′50″ to 73°44′55″ E, respectively (Figure 3). The Siwalik Group is predominantly composed of interchanging sandstone and argillaceous material beds [39]. Overall, the Siwalik Group consists of molass-type sediments of clastic origin. The lithology consists of variegated colour clays with minor sandstone at the base (Chinji Formation), which is superimposed by abundant sandstone with insignificant clays (Nagri Formation). This is aided by sandstone and clay repetitions (Dhok Pathan Formation), which are shadowed by a clay, sandstone, and conglomerate arrangement (Soan Formation) in the upper part of the group. Geologically, the research area is located in the core of the Hazara-Kashmir Syntaxis (HKS) (Figure 1). The HKS consists of various overlapping thrust sheets and is composed of Precambrian to Mesozoic Formations that have been thrust over molasses deposits [15,17]. The Indo-Gangetic alluvium covers Neogene molasse deposits to the south of the Himalayan Frontal Thrust (HFT). The Sub-Himalayan rocks are constrained from the north by the Main Boundary Thrust (MBT) (Figure 1). The MBT separates the rocks of the Sub-Himalayan region from the rocks of the Lesser Himalayan region, while the Main Central Thrust (MCT) divides the rocks of the Lesser Himalayan

region from the rocks of the Higher Himalayan region (Figure 2). The Lesser Himalayan rocks are incorporated by metamorphic rocks of low grade to high grade containing facies ranging from greenschist to amphibolite type facies [40]. The Lesser Himalayan Crystalline refers to these high-grade granitic intrusions and metamorphic rocks [41]. The rocks of the Higher Himalaya contain igneous intrusive rocks (granites) and high-grade metamorphic (gneisses) in the lower unit, whereas metamorphic rocks in the upper unit generally include quartzites and carbonates from the Tethyan deposits [2]. The Siwalik Group in the eastern Nepal Himalaya is divided into the Lower, Middle, and Upper Siwaliks based on the sedimentological characteristics [33]. The Lower, Middle, and Upper Siwaliks are equivalent to the Chinji, Nagri-Dhok Pathan, and Soan Formations, respectively.

3. Material and Methods

The current research was conducted in the Mirpur division's Dadyal to Sehnsa regions of Azad Kashmir, Pakistan. Forty representative sandstones and four clay samples were obtained from the research area's outcrops (Figure 3). The geological traverse technique was used to measure the selected section. Individual bed thicknesses, colours, grain size variations, and sedimentary patterns preserved in rocks were carefully measured. Different facies have been identified in the Siwalik Group based on these characteristics (Table 1). To prepare the lithology of the measured section, the field data were plotted using a graphical approach.

Thin sections of selected rock samples were prepared at the Institute of Geology, University of Azad Jammu and Kashmir, Muzaffarabad. Following that, a petrographic study was carried out using a Leica-DM750P Polarizing microscope equipped with a Leica Image Analyzer (LAV). Table 2 shows the results of the modal mineralogical composition performed using the Gazzi [42] point-counting technique. The triangle classification and origin discrimination diagrams of sandstone were plotted using Origin Pro 6.1 software based on these petrographic data.

The mineralogy of four clay samples from the Siwalik Group was examined using the XRD technique. These XRD investigations were carried out at the University of Peshawar's Centralized Resource Laboratory. Before being bombarded with X-rays, the samples were crushed into a fine powder and then fixed to the slide. XRD studies were performed using an X-ray diffractometer and the XPERT PRO modal. This technique comprises the following components: Anode = Cu, Cu K-Alpha1 = 1.540598 Å, Cu K-Alpha2 = 1.544426 Å, Current = 30 mA, Voltage = 40 Kv, Divergent slit = Fixed – 1.52 mm, Receiving slit = 0.1 mm, Scan range = 10–80, Scan axis = Gonio, Scan type = Continuous, Scan step size = 0.01, Time per step = 0.25. The mineral identification in the clays sample was done using the Jade 6 programme. The shale minerals were obtained using the XRD procedures of Goldsmith and Graf [43] and Goldsmith and Heard [44].

Table 1. Description and interpretation of the Siwalik Group facies association (FA) along Dadyal to Sehnsa area of Mirpur division, Pakistan (Modified after [45,46]).

Facies Association	Major Lithofacies Types	Stratigraphic Unit of the Siwalik Group	Depositional Environment
FC1	St, Fm, Fl	Lower part of Chinji Formation	Fine grained meandering system
FC2	St, Sr, Sh, Fl, Fm	Upper part of Chinji Formation	Flood flow dominated meandering system
FN3	St, Sr, Sh	Lower part of Nagri Formation	Sandy meandering system
FN4	St, Sp, Sr, Sh	Upper part of Nagri Formation	Deep sandy braided system
FD5	St, Sp, Gt, Fms	Dhok Pathan Formation	Shallow braided system
FS6	Gp, Gt, Gh	Lower part of Soan Formation	Gravelly braided system
FS7	Gp, Gh, St, Fm	Upper part of Soan Formation	Debris flow dominated alluvial fans system

Table 2. Modal mineralogical compositions of Siwalik Group of core of HKS.

Modal Mineralogical Composition		Chinji Formation						Nagri Formation										Dhok Pathan Formation										Soan Formation																
		DC-01	DC-02	DC-03	DC-04	DC-05	DC-06	DC-07	DN-08	DN-09	DN-10	DN-11	DN-12	DN-13	DN-14	DN-15	DN-16	DN-17	DN-18	DN-19	DN-20	DD-21	DD-22	DD-23	DD-24	DD-25	DD-26	DD-27	DD-28	DD-29	DD-30	DD-31	DD-32	DD-33	DD-34	DD-35	DD-36	DD-37	DD-38	DD-39	DD-40			
Quartz	Monocrystalline Quartz	Qnu	16	14	12	13	15	12	14	15	17	16	16	14	17	16	14	16	18	20	19	17	16	19	18	16	17	18	17	20	22	21	22	18	21	23	25	10	12	15	17	15		
		Qu	3	2	4	5	4	3	5	4	5	4	5	6	5	3	6	5	6	4	3	5	6	5	6	5	4	5	6	5	4	5	3	4	3	3	4	3	2	3	3	4		
	Polycrystalline Quartz	2-3 grains	1	2	1	2	2	1	3	4	3	2	3	4	3	4	3	3	2	2	4	2	3	3	4	4	3	2	3	4	2	2	2	3	2	3	2	1	2	1	2	1		
		>3 grains	4	4	3	3	4	5	2	6	6	8	5	6	7	8	6	5	5	4	5	6	7	6	6	7	6	7	5	4	4	6	4	5	6	4	4	5	4	3	2	3		
Feldspar	Plagioclase	5	5	7	8	7	6	5	2	3	3	3	2	3	5	4	5	4	4	6	4	3	2	4	4	3	2	3	4	3	3	5	4	3	2	3	8	8	9	8	7			
	Microcline	2	3	3	2	1	2	1	1	1	1	2	1	-	1	-	2	1	-	-	1	1	1	2	1	1	1	2	1	-	1	-	1	-	2	1	2	1	3	2	1			
	Perthite	1	2	1	2	2	4	4	3	2	2	1	2	2	3	3	2	1	3	2	2	2	1	1	1	1	2	1	2	3	2	3	2	2	1	2	1	2	1	1	2			
	Orthoclase	1	1	2	2	2	3	2	2	1	1	1	2	3	2	3	2	3	2	3	1	1	2		2	2	1	1	3	2	1	2	2	1	2	-	2	1	2	2	1			
	Microcline-Perthite	3	2	2	1	1	-	-	3	2	1	3	2	-	-	1	-	-	1	-	-	1	1	1	1	1	1	2	2	-	1	-	-	-	1	-	-	2	1	-	-	1		
Rock Fragments	Igneous	Volcanic (Basalt)	13	14	13	11	9	12	10	7	6	7	6	9	7	6	7	6	6	5	7	8	8	7	7	6	8	8	9	7	8	9	6	7	8	6	8	6	8	11	8	7		
		Volcanic (Rhyolite)	3	7	4	6	5	5	6	11	12	14	11	12	11	9	12	10	13	13	12	13	4	4	3	4	4	5	5	5	4	4	4	4	4	4	4	4	2	3	3	3	4	
		Plutonic (Granite)	-	1	1	-	1	1	1	2	2	2	2	3	2	3	1	2	1	1	2	2	1	1	-	2	1	2	-	1	-	1	-	2	2	1	1	2	1	1	2	1	2	1
	Metamorphic	Slate	1	-	1	-	1	-	1	-	Tr.	1	1	1	1	-	1	-	1	-	-	1	1	Tr.	1	Tr.	1	-	-	-	-	1	-	-	1	1	1	1	1	Tr.	1	2	2	
		Phyllite	2	3	2	2	3	2	1	3	2	1	1	2	2	3	2	3	2	2	3	2	1	1	1	2	1	2	1	2	2	1	2	2	1	2	2	1	2	2	1	2	3	2
		Schist (T)	9	7	7	8	6	8	7	6	8	7	8	7	9	8	8	9	7	8	7	9	4	6	5	7	6	5	6	5	4	5	6	5	6	5	6	5	5	11	13	10	11	12
		Quartz Mica Schist	6	4	4	5	4	6	4	4	5	4	4	4	6	5	4	6	5	6	4	5	2	3	2	3	4	3	4	3	3	3	4	3	4	3	4	3	4	7	9	7	6	8
		Quartz Schist	3	2	2	3	2	2	2	3	2	2	1	2	3	3	3	2	2	3	2	2	2	2	2	2	2	1	2	2	1	1	2	1	2	2	2	1	3	2	3	3	4	
Graphitic Schist	-	1	1	-	-	-	1	-	-	1	2	2	1	-	1	-	-	-	-	-	2	Tr.	1	1	2	1	-	-	1	-	-	1	-	-	-	-	-	1	2	-	2	-		
Gneisse	-	-	-	-	1	1	-	1	2	1	-	2	1	2	1	2	1	1	2	1	1	1	Tr.	-	Tr.	-	-	1	1	-	1	1	-	1	1	-	1	Tr.	1	1	1	1		

4. Results and Discussion

4.1. Field Study

The rocks in the research region were from the Siwalik Group. Sandstone, siltstone, mudstone, shale, clay, and conglomerates were among the exposed rocks. The Chinji Formation sandstone is fine-grained, cross-bedded, and grey to ash grey in colour (Figure 4a). In addition to sandstone, the Chinji Formation contains bioturbated mudstone and variegated coloured shale (Figure 4b). The Nagri Formation is composed of dark greyish to grey sandstone, finer to medium-grained, and dark maroon to reddish shale. Flaser bedding (Figure 4c), plumose structures (Figure 4c), intraformational clasts (Figure 4d), cross-bedding (Figure 4e), and salt and pepper texture characterizes the Nagri Formation sandstone. Clasts of quartzite, volcanic, and clastic rocks are also observed in the Nagri Formation (Figure 4f). The Dhok Pathan Formation is composed of dark grey to brownish, medium- to coarse-grained sandstone with ripple marks, cross bedding (Figure 4g), load casts (Figure 4g), syn-depositional folding (Figure 4h), pebble imbrications, and micro conglomerate lenses (Figure 4i). The Dhok Pathan Formation shale is dark brownish in colour (Figure 4j). Fine- to medium-grained greyish sandstone, polymict conglomerate, and dark reddish shale comprise the Soan Formation. In comparison to the upper part of the Soan Formation, the lower part comprises more sandstone and compacted conglomerate (Figure 4k,l).



Figure 4. Photograph showing (a) fine-grained ash grey cross-bedded sandstone of Chinji Formation; (b) variegated coloured shale of Chinji Formation; (c) flaser bedding and plumose structure in Nagri Formation; (d) intraformational clasts in sandstone of Nagri Formation; (e) cross bedding in sandstone; (f) clasts of volcanic, quartzite and sandstone; (g) cross bedding and load casts; (h) syn-depositional folding; (i) intraformational microconglomerate bed in sandstone; (j) flaser bedding and dark brownish shale; (k) conglomerate and shale of Soan Formation; (l) polymict conglomerate and sandstone of Soan Formation.

Facies Analysis

The descriptive lithological log of the analyzed section has been prepared to represent a typical upward progression of river refining. In the research region, the thicknesses of the Chinji, Nagri, Dhok Pathan, and Soan Formations are 750 m, 1950 m, 3850 m, and 350 m, respectively (Figure 5). In the Siwalik Group, seven major facies assemblages were identified based on lithology and sedimentary structure accumulation. The Miall [45] and Miall [46] lithofacies code and architectural features were used. Table 1 shows the major types of lithofacies, their stratigraphic units, and depositional conditions. The following are descriptions of the facies observed in the studied section:

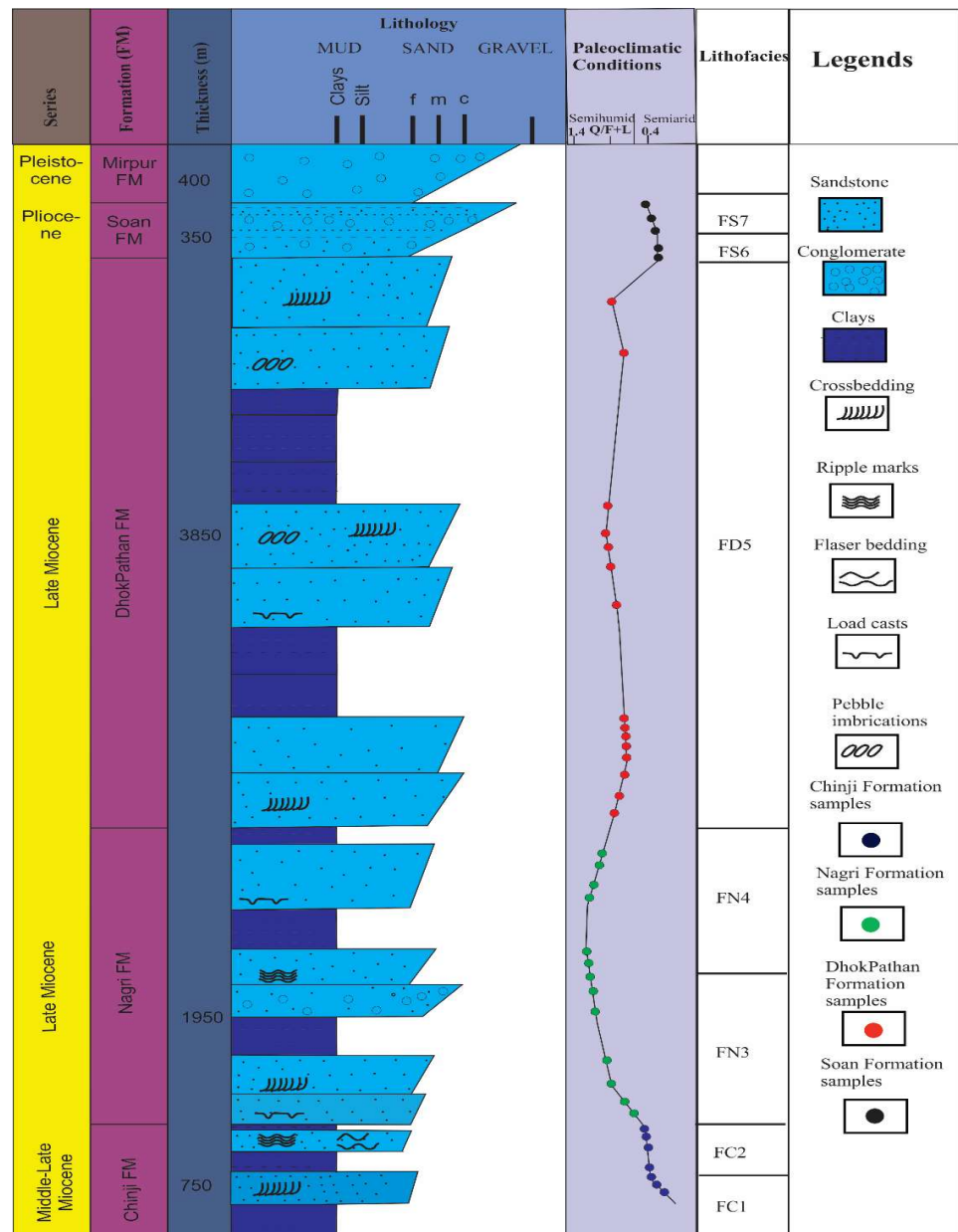


Figure 5. Log showing the lithology of Dadyal to Sehnsa area of Mirpur division.

The FC1 and FC2 facies assemblages are present in the Chinji Formation. The FC1 type facie exists at the base of the Chinji Formation and is characterized by thick stratified ash grey fine-grained sandstone (St, 0.4 to 1.2 m thick) intercalated with mudstone (Fm, 0.8 to 1.7 m thick) and occasionally thin mudstone beds (Fl) (Figure 4a). The sandstone beds have been eroded marginally from the bottom (Figure 4a). Because of the presence of variegated

coloured shale and thick stratified (Fm) mudstone layers in fine-grained sandstone layers, this type of facies results from a fine-grained meandering system. The presence of cross bedded sandstones and a higher proportion of mudstone indicates that they were deposited by meandering rivers with high sinuosity [45,47]. The presence of finer sandstone and mudstone at the top of the upward fining progression indicates deposition that occurred under calm conditions [47,48]. The FC2 type facies is found in the upper section of the Chinji Formation and is distinguished by fine- to medium-grained grey sandstone (St) interbedded with fine-grained muddy sandstone (Sh) and variegated coloured shales (Fm, Fl), (Figure 4b). Finer-grained sandstone is often thin- to thick-bedded (0.3 to 1.9 m). Beds of medium-grained sandstone can be up to 3.7 m thick and include trough cross-stratifications (St). The fine muddy sandstone (Sh) beds are normally 0.3 to 1.9 m thick, whereas the shale beds are 1 to 2 m thick. Flooded conditions in a meandering river system dominate this type of facies [45,47]. The presence of thin, muddy sandstone (Sh) layers within fine- to medium-grained sandstone is thought to be the result of sequential flood episodes. Suspension and weak currents resulted in fine-grained sandstone (Sr) and sandy laminated mudstone (Fl) [47].

There are two types of facies assemblages in the Nagri Formation: FN3 and FN4. The FN3 type facies assemblages are located in the lower Nagri Formation and is composed of medium- to coarse-grained, thick-bedded, dark greyish sandstone mixed with mudstone and muddy sandstone. Channel deposits are represented by sandstone beds with medium to coarse grain size, which show intraformational clasts and cross-stratification (St). Muddy sandstone (Sh) with flaser bedding and plumose structures is interbedded with shale. Sandstone beds are typically 1 to 5 m thick and can reach up to 7 m in thickness, while shale beds are 1 to 3 m thick (Figure 4c,d). A meandering river and flood-flowing channels also contributed to this facies ensemble. This is shown by the presence of sandstone with horizontally accreted cross-stratification and diverse mudstone/shale beds [47,48]. The FN4 facies assemblage occurred in the middle and upper parts of the Nagri Formation (Figure 4e,f), and was distinguished by the presence of medium- to coarse-grained thick-bedded sandstone and shale of dark greyish colour. Trough cross-stratification is visible in the sandstone beds (St). Individual sandstone beds range in thickness from 1 to 8 m, whereas pebbly sandstone beds range in thickness from 0.7 to 4 m. There are rounded to subrounded volcanic, sandstone, siltstone, shale, and quartzite pebbles. Quartzite clasts with diameters ranging from 1 to 8 cm are abundant. Because of the deep, sandy, braided river channel, the facies assemblage with massive bedded sandstone of downstream and horizontal accretionary design was deposited [47]. The presence of intraformational mud and sandstone clasts at the base of each fluvial progression represents bank cut constituents formed during the channel's adjacent movement. The mutual existence of thick fining upward orders and the manifestation of pebbly sandstone beds and dense units of sandstone (St, Sp) having erosional bases proposed that the channel flows were deep.

The Dhok Pathan Formation is distinguished by the presence of coarse- to very coarse-grained thick-bedded sandstone, as well as subsidiary layers of dark grey shale and pebbly sandstone. It is further distinguished by the presence of micro conglomerates, trough stratified gravel (Gt), and an abundance of thick-bedded and pebbly sandstone. Sandstone deposits are trough cross-stratified (St), with load casts and syn-depositional folding (Figure 4g,h). Syn-depositional folding is a deformational sedimentary structure that is often formed as a result of earthquakes triggered by active fault movement. The grain structure of sensitive sand layers breaks down due to the intense shock of seismic waves, causing liquefaction and resulting in the syn-depositional sedimentary structure in the Dhok Pathan Formation. Every fine upward progression begins with coarser sandstone strata and progresses to shale with thicknesses ranging from 8 to 14 m. A shallow, sandy, braided river channel produced the facies assemblage [49]. This is characterized by less obvious fining upward progression, pebbly sandstone, and coarse-grained cross-stratified sandstone beds.

The Soan Formation also represents two facies assemblages, FS6 and FS7. The FS6 facies assemblage is located in the lower Soan Formation (Figure 4k) and is distinguished by the presence of clast-supported conglomerate with minor amounts of dark greyish shale and reddish-brown sandstone. Imbrication and planar cross-stratification are observed in clasts (Gp). Conglomerates vary in thickness from 7 to 18 m, whereas interbedded sandstone and shale beds range in thickness from 0.8 to 1.4 m. The presence of diverse bed load gravel clasts suggests that sediments are deposited by the gravelly braided river system [45,47]. The predominance of conglomerate over other rock types indicates that a shallow river system existed at the time of deposition. The Upper Soan Formation (Figure 4l) has the coarsest facies assemblage (FS7), which is composed mostly of angular to subangular shaped, poorly sorted, sandy matrix-supported conglomerates (Gms). The grading in these aggregates is irregular and loosely packed. Conglomerates (Gm) are often subrounded to subangular in shape, clast-supported, and well-sorted, with a lesser extent of dark greyish to brownish-gray shale (Fm) and grey sandstones (St) present. Conglomerate strata range in thickness from 7 to 16 m, while mudstone and sandstone are less than 3 m thick. Clast-supported boulder conglomerates (Gms facies) with poor sorting and disorganized clast structure are the result of rapid deposition in a fluvial channel caused by debris flows from adjacent sources. The presence of thick-bedded, dark greyish mudstone (Fm) indicates the presence of flooding materials. The well-sorted conglomerates (Gm facies) were deposited by a gravelly river system [45,47,48]. The clast-supported conglomerate and sharp contact beds indicate that this facies assemblage formed as a result of heavier debris flows. As a result, FS7 is represented as the debris-dominated braided system deposits. These types of systems are particularly common in alluvial fan systems.

4.2. Sandstone Petrography

All the Siwalik Group sandstone samples studied contain less than 15% matrix and were distinguished as arenites (Table 2). The recalculated modal mineralogical data (Table 3) of quartz, feldspar, and rock fragments were plotted in a QFL plot [50], which concluded that all samples of the Chinji, Nagri, Dhok Pathan, and Soan Formations were feldspathic litharenite, except for a few samples of the Nagri and Dhok Pathan Formations, which are litharenite (Figure 6a). Sandstone from the Chinji, Nagri, and Dhok Pathan Formations was categorized as volcanic arenite, while sandstone from the Soan Formation was classified as phyllarenite (Figure 6b). Recalculated data of QFL plotted on tectonic discrimination diagrams [51] suggest that the sandstones of Siwaliks have been derived from the recycled orogen provenance field (Figure 6c,d).

Table 3. Recalculated detrital modes for the sandstone of Siwalik Group (Petrographic parameters after Ingersoll and Suczek [52]. Where Qt = Total quartz, Qm = Monocrystalline quartz, Qp = Polycrystalline quartz, F = Feldspar, P = Plagioclase, K = Alkali feldspar, L = Lithics, Lt = Total lithics, Lm = Metamorphic lithics, Lv = Volcanic lithics, Ls = Sedimentary lithics, Lvm = Total volcanic and metavolcanic lithics, Lsm = Total sedimentary and metasedimentary lithics, Rs = Sedimentary lithics, Rm = Metamorphic lithics, Rg = Granite lithics.

Sample No.	QtFL%			QmFLt%			QmPK%			LmLvLs%			QpLvmLsm%			RgRmRs%		
	Qt	F	L	Qm	F	Lt	Qm	P	K	Lm	Lv	Ls	Qp	Lvm	Lsm	Rg	Rm	Rs
DC-1	40.7	20.3	39.0	32.2	20.3	47.5	61.3	16.1	22.6	34.3	45.7	20.0	17.9	57.1	25.0	0	63.2	36.8
DC-2	35.5	21.0	43.5	25.8	21.0	53.2	55.2	17.2	27.6	27.2	56.6	16.2	18.2	63.6	18.2	5.9	58.8	35.3
DC-3	31.7	23.8	44.5	25.4	23.8	50.8	51.6	22.6	25.8	31.6	44.7	23.7	12.5	53.1	34.4	4.6	54.5	40.9
DC-4	35.4	21.5	43.1	27.7	21.5	50.8	54.6	24.2	21.2	29.0	44.7	26.3	15.2	51.5	33.3	0	52.4	47.6
DC-5	41.7	21.7	36.6	31.7	21.7	46.6	59.4	21.9	18.7	33.3	42.4	24.3	21.4	50.0	28.6	5.0	55.0	40.0
DC-6	34.4	24.6	41.0	24.6	25.4	50.0	50.0	20.0	30.0	35.2	45.9	18.9	19.4	54.8	25.8	4.8	61.9	33.3
DC-7	39.3	19.7	41.0	31.1	19.7	49.2	61.3	16.2	22.5	29.4	47.1	23.5	16.7	53.3	30.0	5.3	52.6	42.1

Table 3. Cont.

	Sample No.	QtFL%			QmFLt%			QmPK%			LmLvLs%			QpLvmLsm%			RgRmRs%			
		Qt	F	L	Qm	F	Lt	Qm	P	K	Lm	Lv	Ls	Qp	Lvm	Lsm	Rg	Rm	Rs	
Nagri Formation	DN-8	41.4	15.7	42.9	27.1	15.7	57.2	63.3	6.7	30.0	30.0	45.0	25.0	25.0	45.0	30.0	8.3	50.0	41.7	
	DN-9	46.3	13.4	40.3	32.8	13.4	53.8	70.9	9.7	19.4	33.3	46.2	20.5	25.0	50.0	25.0	8.7	56.5	34.8	
	DN-10	43.4	11.6	45.0	29.0	11.6	59.4	71.4	10.7	17.9	26.8	51.2	22.0	24.4	51.2	24.4	9.1	50.0	40.9	
	DN-11	43.9	15.2	40.9	31.8	15.2	53.0	67.7	9.7	22.6	32.5	45.9	21.6	22.8	48.6	28.6	9.1	54.5	36.4	
	DN-12	44.8	13.4	41.8	29.9	13.4	56.7	69.0	6.9	24.1	32.5	52.5	15.0	26.3	55.3	18.4	13.6	59.1	27.3	
	DN-13	47.8	11.9	40.3	32.8	11.9	55.3	73.3	10.0	16.7	35.0	45.0	20.0	27.0	48.7	24.3	8.4	58.3	33.3	
	DN-14	46.3	16.4	37.3	28.4	16.4	55.2	63.3	16.7	20.0	34.2	39.3	26.5	32.4	40.5	27.1	11.5	50.0	38.5	
	DN-15	43.3	17.9	38.8	29.9	17.9	52.2	64.5	12.9	22.6	31.6	50.0	18.4	25.7	54.3	20.0	5.0	60.0	35.0	
	DN-16	45.3	17.2	37.5	32.8	17.2	50.0	65.6	15.6	18.8	36.8	42.1	21.1	25.0	50.0	25.0	8.3	58.3	33.4	
	DN-17	44.9	13.1	42.0	34.8	13.0	52.2	72.7	12.1	15.2	30.0	47.5	22.5	19.4	52.8	27.8	4.6	54.5	40.9	
	DN-18	44.8	14.9	40.3	35.8	14.9	49.3	70.6	11.7	17.7	28.9	47.4	23.7	18.2	54.5	27.3	4.8	52.3	42.9	
	DN-19	44.9	15.9	39.2	31.9	15.9	52.2	66.6	18.2	15.2	30.8	48.7	20.5	25.0	52.8	22.2	9.1	54.5	36.4	
	DN-20	45.5	12.1	42.4	33.4	12.1	54.5	73.3	13.3	13.4	31.7	51.2	17.1	22.2	58.3	19.5	9.1	59.1	31.8	
	Dhok Pathan Formation	DD-21	56.2	14.0	29.8	38.6	14.0	47.4	73.3	10.0	16.7	29.2	50.0	20.8	37.1	44.4	18.5	7.7	53.8	38.5
		DD-22	57.9	12.3	29.8	42.1	12.3	45.6	77.4	6.5	16.1	36.0	44.0	20.0	34.6	42.3	23.1	6.7	60.0	33.3
		DD-23	57.6	13.6	28.8	40.7	13.5	45.8	75.0	12.5	12.5	33.3	41.7	25.0	37.1	37.0	25.9	0	57.1	42.9
		DD-24	57.1	16.1	26.8	37.5	16.1	46.4	70.0	13.3	16.7	37.5	41.7	20.8	42.3	38.5	19.2	12.5	56.2	31.3
		DD-25	53.6	14.3	32.1	37.5	14.3	48.2	72.5	10.3	17.2	30.7	46.2	23.1	33.4	44.4	22.2	6.7	53.3	40.0
		DD-26	55.2	13.8	31.0	39.7	13.8	46.5	74.2	6.5	19.3	28.0	52.0	20.0	33.3	48.1	18.6	14.3	50.0	35.7
		DD-27	50.8	14.8	34.4	37.7	14.8	47.5	71.9	9.4	18.7	28.6	50.0	21.4	27.6	48.3	24.1	0	57.1	42.9
DD-28		55.0	16.7	28.3	41.6	16.7	41.7	71.4	11.4	17.2	32.0	48.0	20.0	32.0	48.0	20.0	7.1	57.2	35.7	
DD-29		53.3	15.0	31.7	43.3	15.0	41.7	74.3	8.6	17.1	28.0	48.0	24.0	24.0	48.0	28.0	0	53.8	46.2	
DD-30		57.6	11.9	30.5	44.0	11.9	44.1	78.8	9.1	12.1	30.8	50.0	19.2	30.8	50.0	19.2	7.1	57.2	35.7	
DD-31		55.4	17.8	26.8	44.6	17.9	37.5	71.4	14.3	14.3	37.5	41.7	20.8	28.6	47.6	23.8	0	64.3	35.7	
DD-32		53.6	16.1	30.3	39.3	16.1	44.6	71.0	12.9	16.1	29.2	45.8	25.0	32.0	44.0	24.0	13.3	46.7	40.0	
DD-33		56.1	12.3	31.6	42.1	12.3	45.6	77.4	9.7	12.9	37.1	44.4	18.5	30.7	46.2	23.1	11.8	58.8	29.4	
DD-34		57.9	12.3	29.8	45.6	12.3	42.1	78.8	6.0	15.2	32.0	40.0	28.0	29.2	41.7	29.1	6.2	50.0	43.8	
DD-35		58.3	10.0	31.7	48.3	10.0	41.7	82.8	8.6	8.6	29.6	44.5	25.9	24.0	48.0	28.0	6.3	50.0	43.7	
Soan Formation		DS-36	36.6	28.8	34.6	25.0	28.8	46.2	46.4	28.2	25.0	51.6	24.2	24.2	25.0	33.3	41.7	7.5	62.9	29.6
	DS-37	37.7	24.5	37.8	26.5	24.5	49.0	51.9	29.6	18.5	47.1	32.3	20.6	23.1	42.3	34.6	4.1	66.7	29.2	
	DS-38	36.1	24.6	39.3	29.5	24.6	45.9	54.5	27.3	18.2	39.5	36.8	23.7	14.3	50.0	35.7	4.0	60.0	36.0	
	DS-39	44.4	24.1	31.5	37.0	24.1	38.9	60.6	24.2	15.2	50.0	32.3	17.6	19.4	52.4	28.2	8.0	68.0	24.0	
	DS-40	41.8	21.8	36.4	34.5	21.8	43.7	61.3	22.6	16.1	48.6	29.8	21.6	16.7	45.8	37.5	3.7	66.7	29.6	
Mean Value	46.8	16.9	36.3	34.6	16.9	48.5	67.0	14.4	18.6	33.7	44.6	21.7	25.5	48.6	25.9	6.6	56.6	36.8		
Standard Deviation (S.D)	7.8	4.6	5.4	6.3	4.6	5.1	8.9	6.5	4.7	6.1	6.4	2.9	6.9	6.0	5.7	3.9	5.1	5.4		

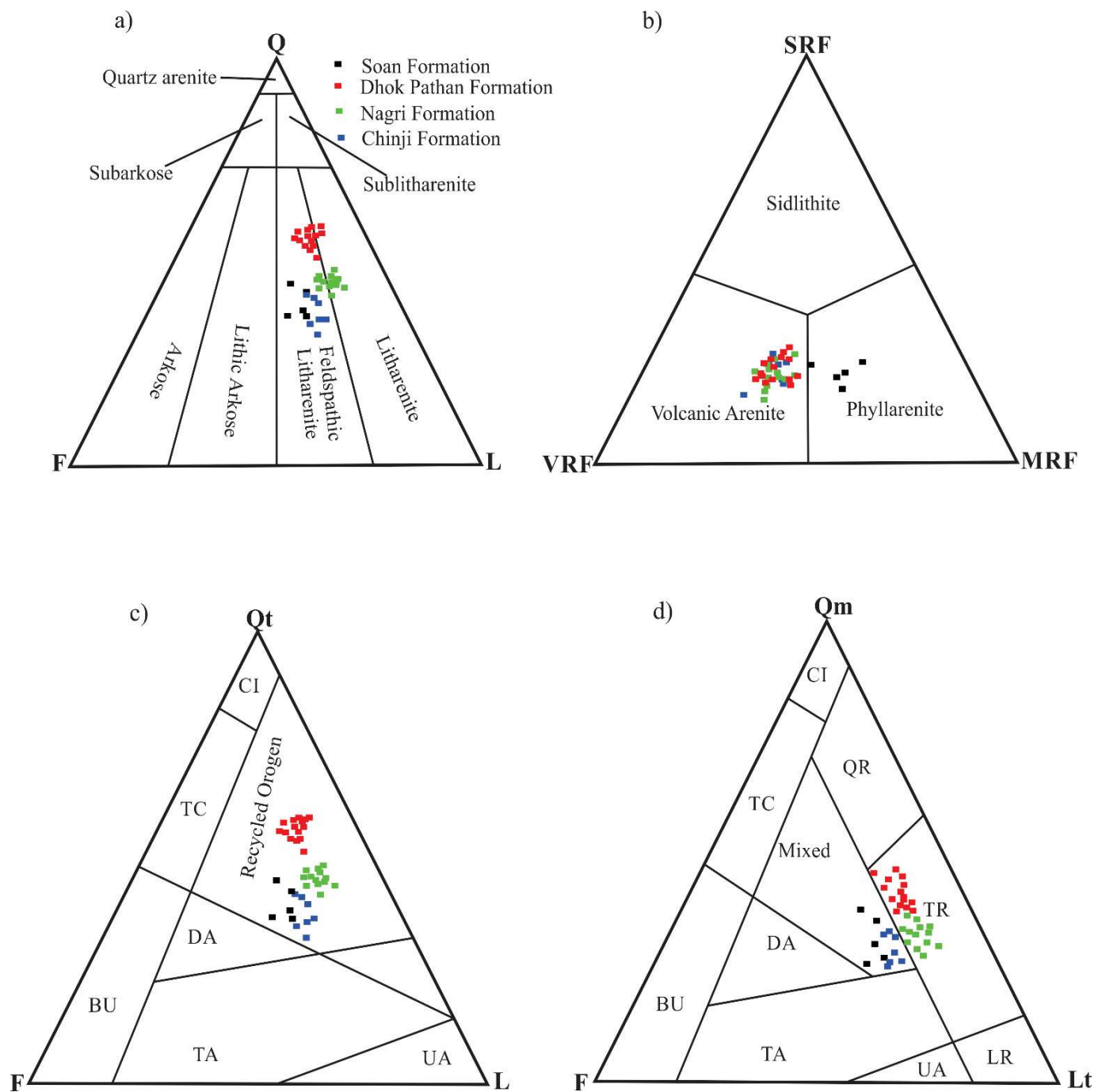


Figure 6. Mineralogical classification (a,b) of the sandstones of the Siwalik Group on the Folk [50] diagram and (c,d) show the standard triangular plots (QtFL and QmFLt) for provenance interpretation of sandstone samples of Siwalik Group (CI = craton interior; TC = transitional continent; BU = basement uplift; DA = dissected arc; TA = transitional arc; UA = undissected arc; QR = quartzose recycling; TR = transitional recycling; LR = lithic recycling).

4.2.1. Feldspathic Litharenite

The feldspathic litharenite of the Chinji and Soan Formations are more cemented than the feldspathic litharenite of the Nagri and Dhok Pathan Formations. Chinji Formation feldspathic litharenite includes 20 to 25% quartz, 12 to 15% feldspar, and 34 to 39% rock fragments, respectively. The Nagri Formation’s feldspathic litharenite comprises 29 to 32% quartz, 8 to 12% feldspar, and 39 to 43% rock fragments, respectively (Table 2). The proportions of quartz, feldspar, and rock fragments in the Dhok Pathan Formation are 30 to

35%, 6 to 10 %, and 24 to 29%, respectively (Table 2). In comparison, the Soan Formation contains 19 to 24% quartz, 12 to 15% feldspar, and 35 to 39% rock fragments, respectively (Table 2). The quartz grains of the Chinji Formation are subangular to subrounded, while the quartz grains in the Dhok Pathan and Soan Formations are subangular to angular. A few grains of monocrystalline quartz are stretched, strained, and rounded in all of these formations. Planer and concavo–convex contacts are common in polycrystalline quartz grains. All feldspathic litharenite consists of clasts of igneous, metamorphic, and sedimentary rocks.

In the Chinji and Dhok Pathan Formations, igneous clasts dominate over the others, but in the Soan Formation, metamorphic clasts predominate over volcanic and sedimentary clasts. Igneous clasts are primarily volcanic (basalt) (Figure 7a), and rhyolite (Figure 7b), with minor plutonic (granite) clasts (Figure 7c). In comparison to rhyolite clasts, basaltic volcanic clasts are abundant. Schist dominates metamorphic clasts, with modest amounts of slate, phyllite, gneisses, and quartzite. Schist clasts predominate over other metamorphic clasts. Sandstone (Figure 7d,e), siltstone, limestone (Figure 7d,e), and dolomite (Figure 7d) are examples of sedimentary clasts, with an abundance of siltstone and limestone clasts. Feldspar of both types (alkali feldspar and plagioclase) was present in all of the samples analyzed. Perthite and orthoclase are abundant in alkali feldspar compared to microcline. In the Chinji and Dhok Pathan Formations, alkali feldspar has a slight advantage over plagioclase, but in the Soan Formation, plagioclase outnumbers alkali feldspar. Plagioclase is usually deformed, fractured, and altered to opaque minerals, including sericite. Biotite, muscovite, monazite (Figure 7f,g), xenotime (Figure 7g), zircon (Figure 7h), tourmaline, and epidote (Figure 7e,g) are the most common accessory minerals, with traces of hornblende and chlorite. Tremolite and orthopyroxene are only observed in trace amounts in the Soan Formation. Muscovite is a highly deformed mineral formed by weathering or diagenesis from biotite (Figure 7i). The matrix varies from 3 to 6% in the Chinji Formation, 2 to 7% in the Nagri Formation, 9 to 13% in the Dhok Pathan Formation and 7 to 10% in Soan Formation (Table 2) and is formed during diagenesis by the alteration of feldspar and rock fragments (slate, schist, and siltstone). Cementing materials in these sandstones is dominantly calcite (Figure 7e) with a minor quantity of ferroan calcite. Calcite varies from 6%–10%, 5%–10%, 7%–12%, and 11%–13% in Chinji, Nagri, Dhok Pathan, and Soan Formations, respectively. The ferroan calcite ranges from 1%–3% in in these sandstones (Table 2).

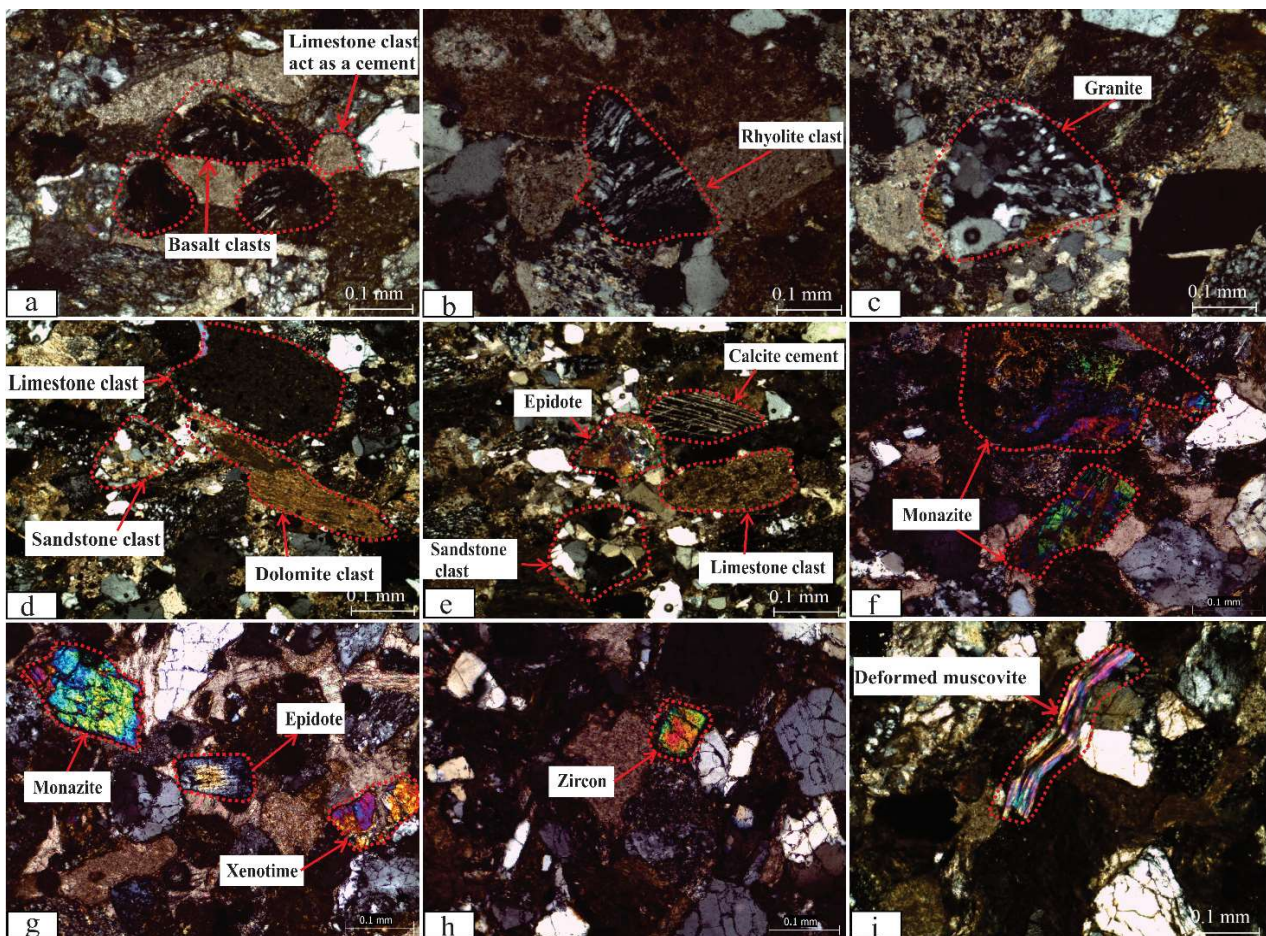


Figure 7. Photomicrographs showing (a) basalt clasts and limestone clasts acting as cementing material, (b) rhyolite clast, (c) granite clast, (d) sandstone, limestone and dolomite clasts, (e) calcite cement, epidote, limestone and sandstone clast, (f) monazite, (g) monazite, xenotime and epidote, (h) zircon, and (i) deformed muscovite.

4.2.2. Litharenite

The Nagri Formation's litharenite sandstones are relatively well cemented. Quartz, feldspar, and rock fragments account for 29 to 32%, 8 to 12%, and 39 to 43% of the total, respectively (Table 2). The percentage of matrix in litharenite varies from 2 to 5%. The quartz grains of Nagri Formation litharenite are mostly angular to sub-angular in form, with a few rounded to subrounded grains. The majority of the quartz grains are monocrystalline (Qm), with a smaller proportion of polycrystalline quartz (Qp) grains (Figure 8a). Phyllite, schist (Figure 8b–d), volcanic (basalt and rhyolite; Figure 8a–c), plutonic (granite), sandstone (Figure 8a), siltstone, and limestone are all present in the litharenite (Figure 8e). In litharenite, clasts of low to medium grade metamorphics (schist) and volcanic rocks composed of basalt and rhyolite predominate over other rock fragments. Rhyolite clasts are more abundant in volcanic fragments than basalt clasts. Plagioclase and alkali feldspar are both present in feldspar. Plagioclase grains exhibit zoning (Figure 8f) and sericite alteration. Perthite, microcline perthite (Figure 8g,h), orthoclase, and microcline are all observed in alkali feldspar. As accessory minerals, muscovite, biotite, monazite (Figure 8g,i), xenotime (Figure 8i), zircon, epidote, and chalcedony (Figure 8e) were reported, along with a trace of tourmaline and chlorite. Calcite is the most prevalent type of cement, with minor amounts of ferroan calcite. Litharenites from the Nagri Formation are volcanic arenite

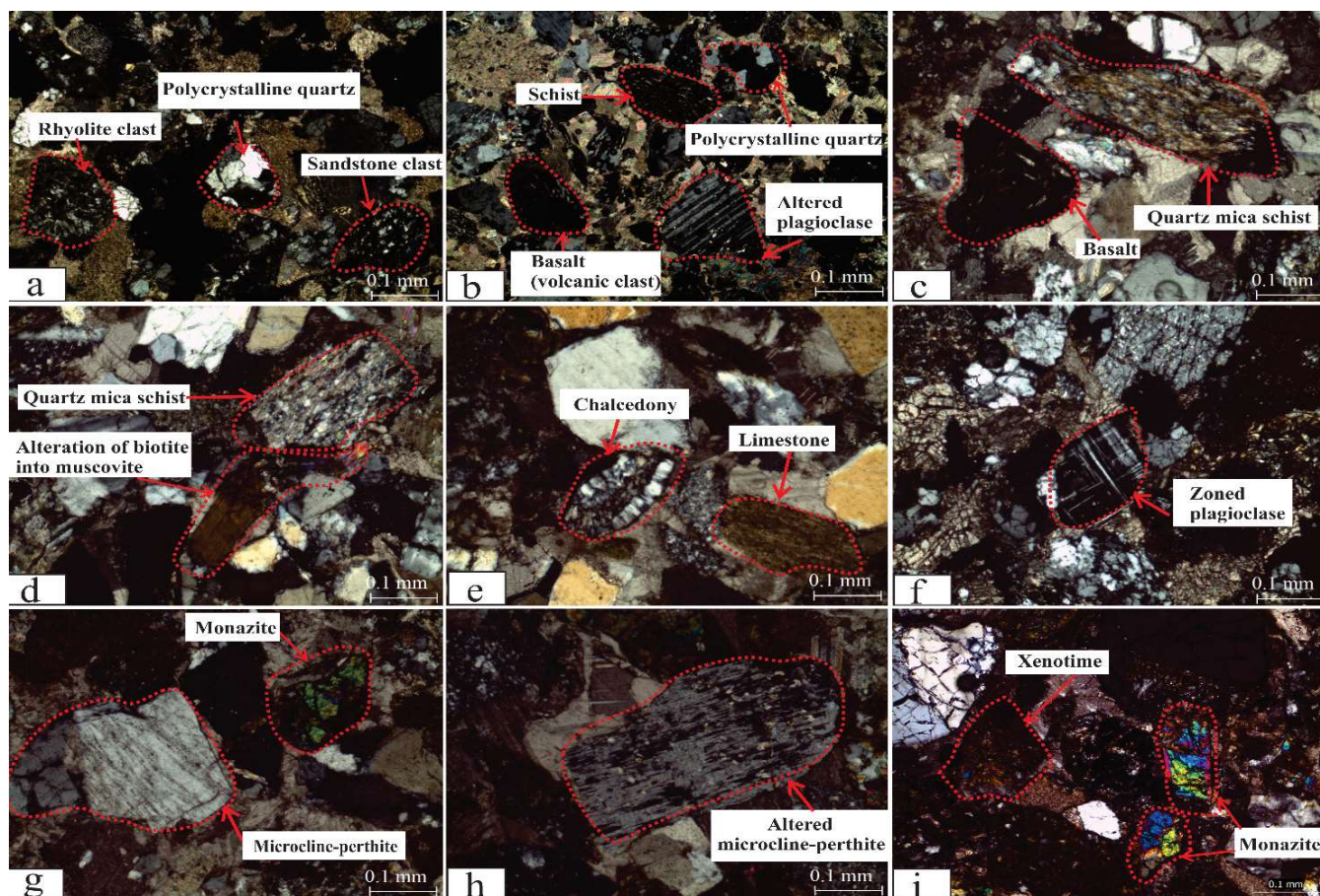


Figure 8. Photomicrographs showing (a) volcanic (rhyolite), polycrystalline quartz and sandstone clast, (b) polycrystalline quartz, schist, volcanic (basalt) clast and altered plagioclase, (c) basalt and quartz-mica schist, (d) quartz-mica schist and alteration of biotite into muscovite, (e) chalcedony and limestone clast, (f) zoned plagioclase, (g) microcline perthite and monazite, (h) altered microcline perthite, and (i) monazite and xenotime.

The sandstone detrital modes are employed to explain compositional variability and the impact of source rock on the Siwalik Group. Poor to moderate sorted Siwalik sandstones are texturally mature. Their average composition fluctuates from lithic to quartzose rich ($Qm34.6 \pm 6.3$ $F16.9 \pm 4.6$ $Lt48.4 \pm 5.1$; Table 3; Figure 9a). The proportion of monocrySTALLINE quartz is 25 to 48% ($QmFLt\%Qm$), lithic fragments range from 37 to 59% ($QmFLt\%Lt$) and feldspar 10 to 28 % ($QmFLt\%F$). In the sandstone, as compared to the plagioclase, the alkali feldspar is more abundant ($Qm67 \pm 8.9$ $P14.3 \pm 6.5$ $K18.6 \pm 4.7\%$; Figure 9b; Table 3). The petrofacies of Siwalik Group sandstone are quartzolithic, which resembles the identical provenance but different paleo-climatic settings. Lithic fragments (aphanitic), ($Lm33.7 \pm 6.1$ $Ls21.6 \pm 2.4$ $Lv44.5 \pm 6.4\%$; Figure 9c; Table 3) include abundant igneous clasts (basalt, rhyolite, and granite), metasedimentary (slate, phyllite, schist, and gneisses), and sedimentary (carbonate rocks, siltstone, and fine-grained sandstone) grains. In the Soan Formation, clasts of basalt and rhyolite are in lesser proportion relative to the metasedimentary/sedimentary clasts. Whereas, in the Chinji, Nagri, and Dhok Pathan Formations, the concentration of basaltic and rhyolite clasts is greater as compared to other clasts (Table 2). As compared to the polycrystalline quartz and sedimentary/metasedimentary clasts, volcanic/metavolcanic fragments are abundant ($Lsm25.9 \pm 5.6$ $Lvm48.6 \pm 6$ $Qp25.3 \pm 6.9$; Figure 9d; Table 3). However, the plutonic fragments relative to the sedimentary and metasedimentary fragments are in negligible quantity ($Rm56.6 \pm 5.1$ $Rs36.8 \pm 5.4$ $Rg6.5 \pm 3.8$; Figure 9e; Table 3).

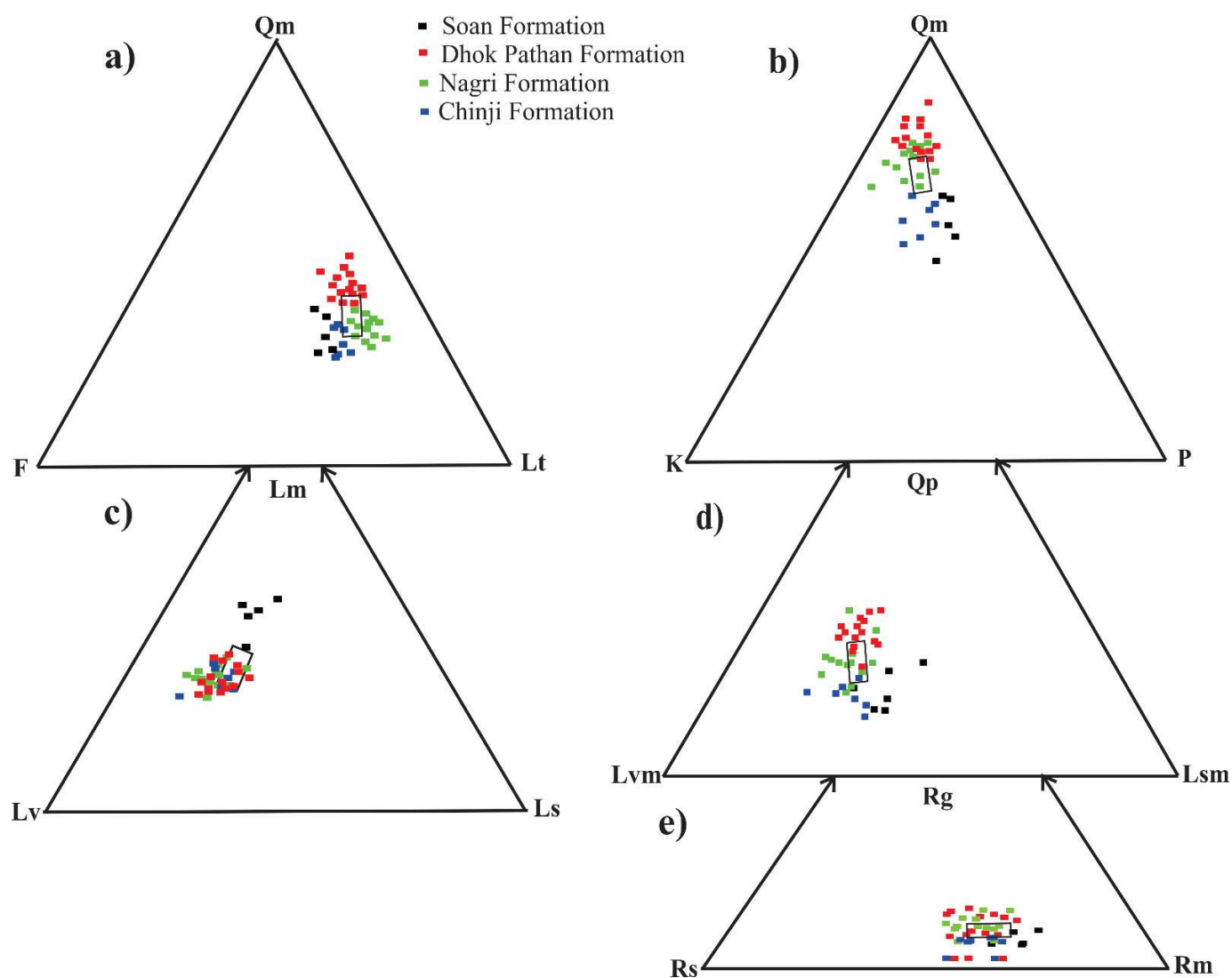


Figure 9. QmFLt (a), QmPK (b), LmLvLs (c), QpLvmLsm (d) and RgRsRm (e) ternary plots for the Siwalik Group. Polygons are one standard deviation on either side of the mean. The modal composition data plotted on the diamond diagram of Basu, et al. [53] indicate the plutonic and metamorphic provenances of middle to upper rank for the sandstone of Siwalik Group (Table 2; Figure 10a). The bivariate log–log plot ($Qp/(F + L)$) against $Q/(F + L)$ reveals that the Chinji and Soan Formations' sandstone are plotted in semi-arid whereas, the sandstone of Nagri and Dhok Pathan Formations are plotted in the semi-humid field (Figure 10b). The weathering index diagrams indicate the majority of sandstone plots fall into the field of $wi = 0$ (Figure 10c) [54,55]. The paleoclimatic condition of the Siwalik Group is interpreted as arid to semi-humid by plotting QFL data on the ternary diagram (Figure 10d) [56].

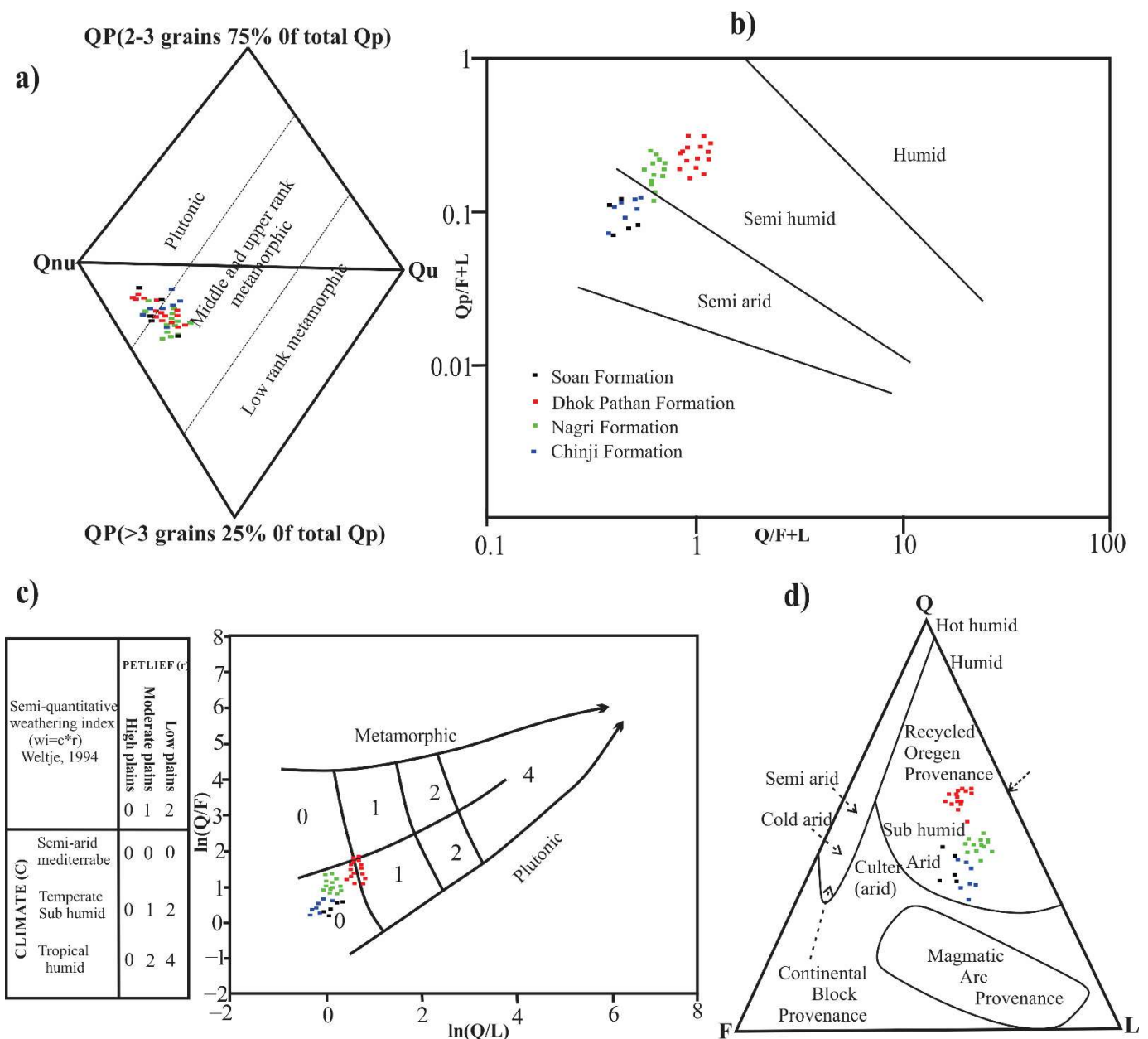


Figure 10. Diagram (a) shows Diamond diagram for interpretation of provenance of Siwalik Group, Diagram (b) showing the paleoclimatic condition of the Siwalik Group and is interpreted based on the plot of the Suttner and Dutta [56] Qp/(F+RF) vs. Q/(F+RF), (c) Weathering diagram and semi-quantitative weathering index after Weltje (1994), (d) interpretation of climatic conditions from QFL ternary diagram for the sandstones of Siwalik Group.

4.3. XRD Analysis

Quartz, goethite, siderite, aragonite, dolomite, muscovite, albite, and hematite have been identified as minerals in the Siwalik Group shale (Figure 11a–d). The presence of quartz and plagioclase (albite) indicates that these shales were formed from granitic rocks. The presence of hematite indicates that micaceous minerals were oxidized during the deposition of shale. Carbonate minerals (siderite, dolomite, and aragonite) indicate that Fe-, Mg-, and Ca-rich fluids migrated from carbonate rocks (limestone and dolomite) and were deposited in Siwalik Group shales. Illite, chlorite-montmorillonite, smectite-montmorillonite, and mica-montmorillonite have been reported as clay minerals in the Siwalik Group shale. The XRD study of the Siwalik Group shale demonstrates that clay minerals vary

in composition. Weathering and erosion of rocks form clay minerals, which include both transported and detrital clays [57]. During chemical weathering, the feldspar content of rocks is released and forms clay minerals such as smectite. Clays include fine-grained mica as well (muscovite and biotite). Illite is a weathering product of feldspar and muscovite that produces white mica (sericite), as indicated by the sericitization of feldspar grains in sandstone petrography [57] (Figure 8b,h). Illite can be found in argillaceous sedimentary rocks as well as certain low-grade metamorphic rocks. Clay minerals were mixed due to the presence of minor amounts of quartz, metal oxides, and organic matter [58]. Because quartz, in comparison to feldspar, is the most resistant mineral, shales of the Siwalik Group contain abundant quartz that has only changed size to clay-sized particles during long-distance transportation. Oxides are observed in the petrographic (Table 2) and XRD analysis (Figure 11a–d) samples of Siwalik Group quartz and metal, resulting in the formation of mixed-layer clays such as chlorite-montmorillonite and smectite-montmorillonite.

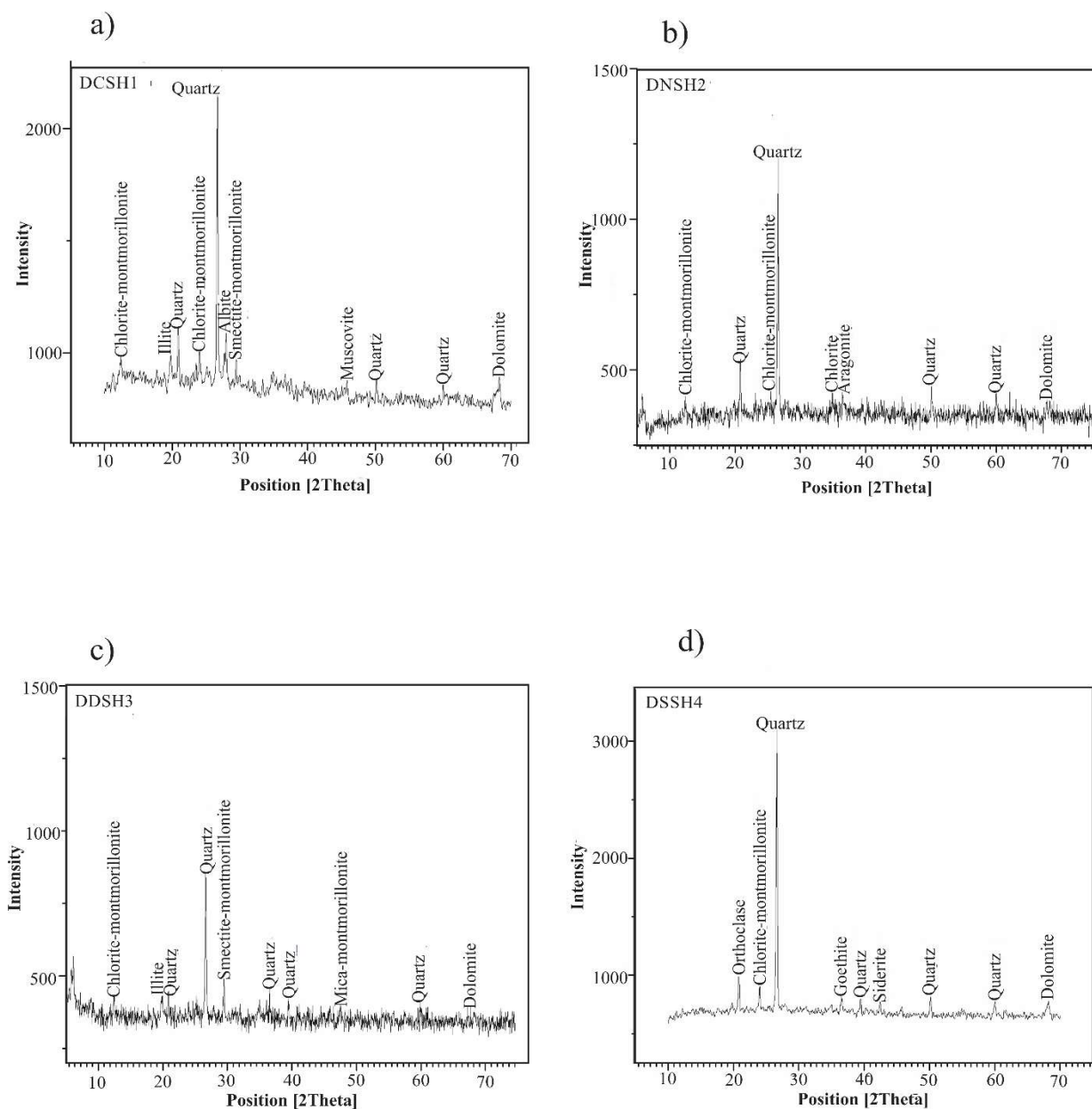


Figure 11. Graphs showing the powder X-ray diffraction pattern of Siwalik Group shales. (a) Chinji Formation, (b) Nagri Formation, (c) Dhok Pathan Formation, and (d) Soan Formation.

4.4. Depositional Environment

The Siwaliks' depositional environment is revealed via field and sedimentological investigations. The Chinji Formation is composed mostly of variegated coloured clays (60%–70%; Figure 4b) and ash grey, fine to medium-grained cross-bedded sandstone (30%–40%; Figure 4a), and is divided into two facies assemblages (FC1 and FC2). The Chinji Formation's FC1 type facie composition (Figure 4a) is distinguished by thick layered ash-grey fine-grained sandstone (St) intercalated with mudstone (Fm) and layers of thin mudstone (Fl). The FC2 type facie assemblage is characterized by fine to medium-grained grey sandstone (St) interbedded with muddy, fine-grained sandstone (Sh) and variegated coloured shales (Fm, Fl). These types of facies indicate that the Chinji Formation was deposited by river meandering flood plain systems [48,59] (Figure 12). These floods occurred as a result of significant rainfall in semiarid conditions during the Chinji Formation's formation [60]. The Nagri Formation is composed mostly of clays (30%–40%) and grey-coloured cross-bedded, thin to thick-bedded, medium to coarse-grained rippling sandstone (60%–70%) with pebble-sized basalt clasts in its upper part, and it is also divided into two facies assemblages (FN3 and FN4) (Figure 4f). The Nagri Formation's FN3 facies assemblage consists of medium to coarse-grained, thick-bedded, dark grey sandstone (St) linked with muddy sandstone (Sh) and mudstone (Figure 4c,d), whereas the FN4 facies assemblage (Figure 4e,f) is identified by the presence of medium to coarse-grained, thick-bedded sandstone (St) and dark grey shale. According to these facies assemblages, the Nagri Formation was deposited by a meandering river into a deep, sandy, braided river system [59,61] (Figure 12). The Dhok Pathan Formation has almost equal proportions of sandstone and clay (Figure 4j). The Dhok Pathan Formation sandstone is thick-bedded to massive, cross-bedded to planar-bedded, medium to coarse-grained, and includes pebble to cobble-sized clasts of basalt, rhyolite, quartzite, sandstone, and limestone. In the study area, the Dhok Pathan Formation contains an FD5 facies assemblage. Thick-bedded sandstone (St; Figure 4g), micro conglomerates (Figure 4i), trough stratified gravel (Gt), and pebbly sandstone are also observed. Because of the presence of the FD5 facies assemblage, the Dhok Pathan Formation was most likely deposited by shallow braided sandy river systems (Figure 12) [59,61]. The Soan Formation, on the other hand, shows a coarsening upward sequence and is composed of clays, sandstones, and conglomerates. The Soan Formation had two facies assemblages (FS6 and FS7) in the studied area. The FS6 facies assemblage (Figure 4k) is distinguished on the basis of clast-supported conglomerate (Gp) with reddish-brown sandstone and, to a lesser extent, dark grey shale. The facies assemblage (FS7) is the coarsest facies association, comprising of sandy matrix supported conglomerates (Gms) and well-sorted conglomerates (Gm), with a minor amount of dark grey to brownish-grey shale (Fm) and grey sandstones (Figure 4l). The Soan Formations were deposited by alluvial fan systems, according to this facies assemblage [45,47,48] (Figure 12). Overall, the Siwaliks are coarsening upward, indicating that they were deposited by a fluvial system (Figure 12).

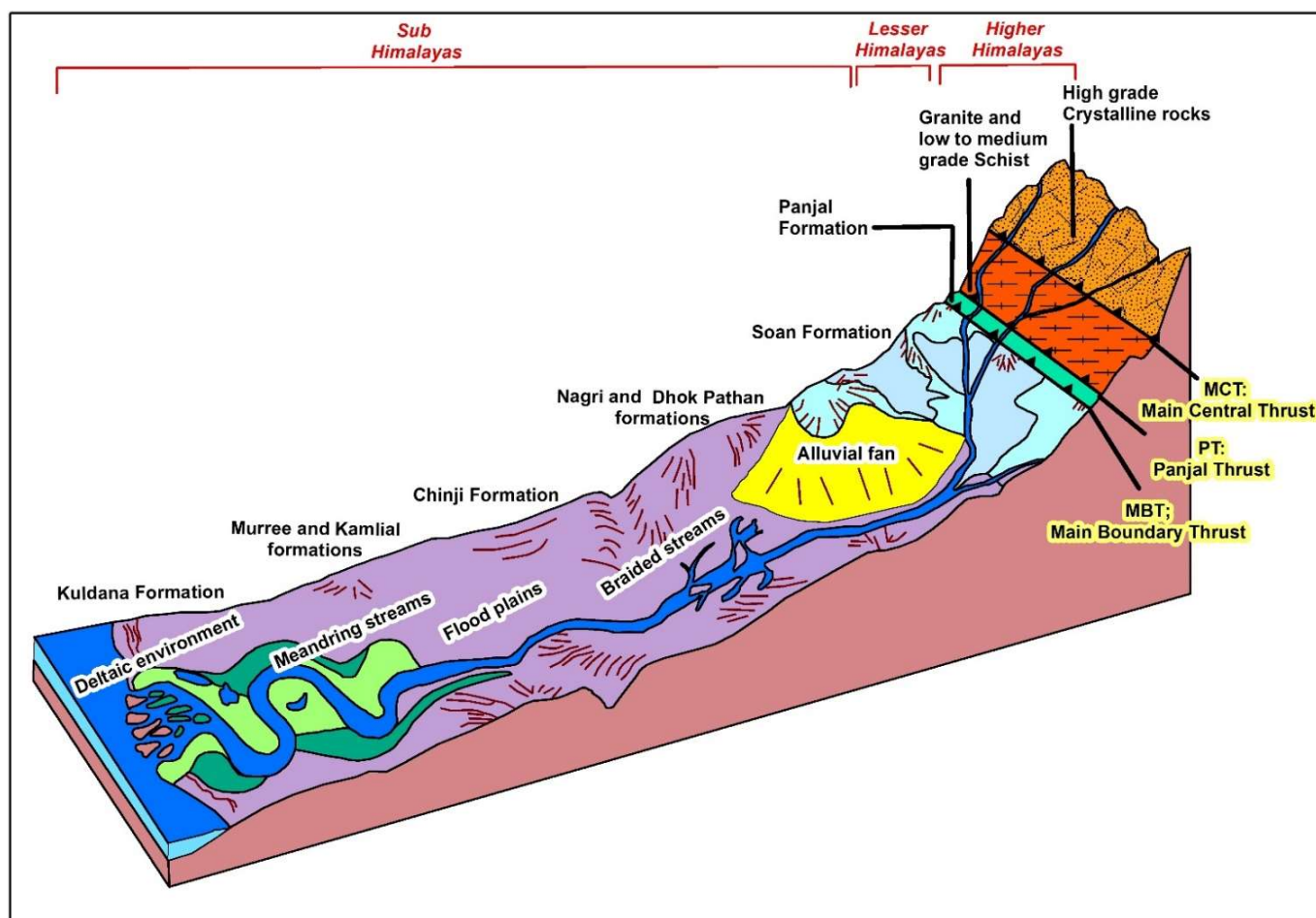


Figure 12. Generalized hypothetical depositional model of Himalayan Mollase based on previously published studies [2,4,20] and this study.

4.5. Provenance and Tectonic Setting of the Siwalik Group

The tectonic discrimination diagrams indicate that the Siwalik sandstones are derived from a recycled orogen provenance field (Figure 6c,d) [29]. Furthermore, the modal composition data plotted on the diamond diagram shows plutonic and metamorphic provenances of middle to upper rank for Siwalik Group sandstone (Table 2; Figure 10a) [39]. The abundance of non-undulatory monocrySTALLINE quartz (Qnu) in the sandstone (Qnu64.46.4 Qu16.34 Qp > 3 19.165) reveals the sandstone's plutonic provenance. The undulatory and polycrystalline quartz grains indicate that they originated from high-grade metamorphic rocks, acidic plutonic rocks, and ancient sandstone origins [37,50]. Orogenic recycling occurred in upper and lower Himalayan areas where these igneous and stratified rocks were subjected to deformation, uplifting, and erosion [2], eventually depositing in the Himalayan Foreland Basin as Siwalik detritus. The petrographic examination also demonstrates that rock fragments found in sandstones vary significantly from base to top. The sandstones of the lower and middle Siwaliks, such as the Chinji and Dhok Pathan Formations, are dominated by volcanic clasts (basalt and rhyolite), while the upper Siwaliks, such as the Soan Formation, are characterized by metamorphic clasts (Table 2). These volcanic clasts in sandstone are most likely from the Panjal Formation [2]. There are fewer plutonic fragments observed in Siwalik sandstones. These plutonic fragments have disintegrated into quartz and feldspar as a result of mechanical weathering. During the Miocene, the Himalayan orogenic belt uplift rates increased significantly [62], exposing igneous, metamorphic, and sedimentary rocks to denudation.

The Kuldana Formation of Middle Eocene-Early Oligocene was deposited during the initial stages of the Himalayan orogeny as a result of the Ceno-Tethys Ocean's regression

and transgression, as revealed by a succession of siliciclastic and non-clastic rocks [4]. The Rawalpindi Group of the Miocene age, which is older than the Siwalik Group, is comprised of the Murree and Kamlial Formations. The Early Miocene Murree Formation was deposited in the Himalayan Foreland Basin by a river meandering system [2,20]. The detritus of rock fragments includes igneous and stratified (sedimentary and metamorphic) rocks, indicating that rock fragments are derived from various sources (Figure 6d). The composition of these sandstone clasts is comparable to that of previous molasses, but the limestone and dolomite clasts are pre-molasses in origin. Both of these pre-molasses locations are in the Sub-Himalayas. These older molasses sandstone clasts indicate that the Siwalik Group formed during the Middle Stage of the Himalayan orogeny.

Because the Siwalik sandstone contains moderate to low amounts of quartz and feldspar, these clasts were deposited by large rivers as a result of collision orogen and foreland uplift origins [63]. Deformed muscovite and biotite flakes show that they are produced from metamorphic rocks or tectonically deformed assemblages, and the presence of epidote and metamorphic clasts suggests a similar origin [64]. The presence of tourmaline indicates that they were formed from pegmatites, granite, schists, or immature sedimentary rocks of the nearby Himalayan orogenic zone [65]. The presence of monazite and xenotime suggest dominantly felsic igneous and metamorphic rocks i.e., slate, phyllite, schist and gneiss [66]. The presence of zircon suggests that the source rocks are both igneous and metamorphic [67].

4.6. Paleoclimatic Conditions

The $Qp/(F + L)$ against $Q/(F + L)$ bivariate log–log plot reveals that the Chinji and Soan Formations' sandstone are plotted in semi-arid whereas, the sandstone of Nagri and Dhok Pathan Formations are plotted in the semi-humid field (Figure 10b). The compositional maturity resulting from $Qp/(F + L)$ and $Q/(F + L)$ is below 0.60 and 3.0, respectively, indicating the poor compositional maturity of sandstone. The weathering index diagrams indicate the majority of sandstone plots fall into the field of $w_i = 0$ (Figure 10c) [2]. This reveals that the sedimentation occurred in high relief with changing climatic conditions from semi-arid, temperate sub-humid, tropical, and humid. The paleoclimatic condition of the Siwalik Group is interpreted as arid to semi-humid by plotting QFL data on the ternary diagram (Figure 10d) [4,68]. The Siwalik sandstones are deposited in a semi-arid to semi-humid climate and reveal low to moderate compositional maturity on the basis of a mean QFL ratio of $46.8 \pm 7.8:16.9 \pm 4.6:36.2 \pm 5.4$ (Table 3). In semi-arid paleoclimatic conditions, floods occurred due to heavy rain and either snow or glacier melting processes [69]. The Chinji Formation was deposited in semi-arid paleoclimatic conditions due to heavy rainfall, whereas the Soan Formation was deposited due to the melting of snow or glacier. The Nagri and Dhok Pathan Formations were deposited in semi-humid paleoclimatic conditions. This is evidenced by the presence of feldspar in lesser quantities as compared to quartz and lithics (Table 2).

5. Conclusions

Based on field observations, facies assemblages, petrographic investigations, and XRD analysis, the following conclusions were reached:

1. The Siwalik Group is deposited in the Himalayan Foreland Basin by meandering to braided stream systems. The Tortonian Chinji Formation is deposited by flood plains, the Zanclean Nagri and Piacenzian Dhok Pathan Formations by braided rivers, and the Gelasian Soan Formation by alluvial fans.
2. The Siwalik Group sandstone is classified as feldspathic litharenite and litharenite. All of the data are presented in ternary discrimination diagrams with recycled orogen provenance fields.
3. The Siwalik Group sandstone contains a significant amount of igneous, metamorphic, and sedimentary rock fragments. The igneous and metamorphic rock clasts originate from lesser and higher Himalayan rocks. The sedimentary rock clasts, on the other

hand, are formed from both earlier molasses, such as the Rawalpindi Group, and pre-molasses rocks (Tethyan sediments). These earlier molasses sandstone clasts identified in the Siwalik Group sandstones indicate that they were deposited during the Middle Stage Himalayan orogeny.

4. The Chinji and Soan Formations were deposited in a semi-arid paleoclimatic environment, whilst the Nagri and Dhok Pathan Formations were deposited in a semi-humid paleoclimatic environment.
5. The abundant clay minerals in the shales suggest intense chemical weathering effects on the river meandering system's flood plains throughout their deposition.

Author Contributions: Conceptualization, M.Z. and M.R.K.; Data collection, M.Z., M.R.K. and M.S.M.; Methodology, M.Z., M.R.K. and M.S.M.; Software, M.Z., M.R.K., M.S.M. and H.T.J.; Writing—Original draft preparation, M.Z.; Supervision, M.R.K.; Writing—Review and editing, M.R.K., M.S.M., H.T.J., P.M. and G.K. All authors have read and agreed to the published version of the manuscript.

Funding: This research received no external funding.

Data Availability Statement: Not Applicable.

Acknowledgments: The senior author would like to express gratitude to the Institute of Geology, University of Azad Jammu and Kashmir, Muzaffarabad, Pakistan for providing the opportunity and facility for this research.

Conflicts of Interest: The authors declare no conflict of interest.

References

1. Najman, Y.; Garzanti, E.; Pringle, M.; Bickle, M.; Stix, J.; Khan, I. Early-Middle Miocene paleodrainage and tectonics in the Pakistan Himalaya. *Geol. Soc. Am. Bull.* **2003**, *115*, 1265–1277. [[CrossRef](#)]
2. Mughal, M.S.; Zhang, C.; Du, D.; Zhang, L.; Mustafa, S.; Hameed, F.; Khan, M.R.; Zaheer, M.; Blaise, D. Petrography and provenance of the Early Miocene Murree Formation, Himalayan Foreland Basin, Muzaffarabad, Pakistan. *J. Asian Earth Sci.* **2018**, *162*, 25–40. [[CrossRef](#)]
3. Ali, S.K.; Janjuhah, H.T.; Shahzad, S.M.; Kontakiotis, G.; Saleem, M.H.; Khan, U.; Zarkogiannis, S.D.; Makri, P.; Antonarakou, A. Depositional Sedimentary Facies, Stratigraphic Control, Paleoecological Constraints, and Paleogeographic Reconstruction of Late Permian Chhidru Formation (Western Salt Range, Pakistan). *J. Mar. Sci. Eng.* **2021**, *9*, 1372. [[CrossRef](#)]
4. Bilal, A.; Mughal, M.S.; Janjuhah, H.T.; Ali, J.; Niaz, A.; Kontakiotis, G.; Antonarakou, A.; Usman, M.; Hussain, S.A.; Yang, R. Petrography and Provenance of the Sub-Kuldana Formation: Implications for Tectonic Setting and Palaeoclimatic Conditions. *Minerals* **2022**, *12*, 794. [[CrossRef](#)]
5. Qureshy, M.; Venkatachalam, S.; Subrahmanyam, C. Vertical tectonics in the Middle Himalayas: An appraisal from recent gravity data. *Geol. Soc. Am. Bull.* **1974**, *85*, 921–926. [[CrossRef](#)]
6. Parkash, B.; Sharma, R.; Roy, A. The Siwalik Group Himalayan (molasse)—Sediments shed by collision of continental plates. *Sediment. Geol.* **1980**, *25*, 127–159. [[CrossRef](#)]
7. Goswami, P.K.; Deopa, T. Petrotectonic setting of the provenance of Lower Siwalik sandstones of the Himalayan foreland basin, southeastern Kumaun Himalaya, India. *Isl. Arc* **2018**, *27*, e12242. [[CrossRef](#)]
8. Basharat, M.; Rohn, J.; Ehret, D.; Baig, M.S. Lithological and structural control of Hattian Bala rock avalanche triggered by the Kashmir earthquake 2005, sub-Himalayas, northern Pakistan. *J. Earth Sci.* **2012**, *23*, 213–224. [[CrossRef](#)]
9. Avouac, J.-P.; Ayoub, F.; Leprince, S.; Konca, O.; Helmberger, D.V. The 2005, Mw 7.6 Kashmir earthquake: Sub-pixel correlation of ASTER images and seismic waveforms analysis. *Earth Planet. Sci. Lett.* **2006**, *249*, 514–528. [[CrossRef](#)]
10. Greco, A. Stratigraphy metamorphism and tectonics of the Hazara-Kashmir syntaxis area, Kash. *J. Geol.* **1991**, *8*, 939–965.
11. Baig, M.; Lawrence, R. Precambrian to early Paleozoic orogenesis in the Himalaya. *Kashmir J. Geol.* **1987**, *5*, 1–22.
12. Calkins, J.A.; Offield, T.W.; Abdullah, S.K.M. *Geology of the Southern Himalaya in Hazara, Pakistan and Adjacent Areas*; U.S. Government Printing Office: Washington, DC, USA, 1975.
13. Wadia, D. The syntaxis of the northwest Himalaya: Its rocks, tectonics and orogeny. *Rec. Geol. Surv. India* **1931**, *65*, 189–220.
14. Ashraf, M.; Chaudhary, M. Petrology of lower Siwalik rocks of Poonch area. *Kashmir J. Geol.* **1984**, *2*, 1–10.
15. Bossart, P.; Dietrich, D.; Greco, A.; Ottiger, R.; Ramsay, J.G. The tectonic structure of the Hazara-Kashmir syntaxis, southern Himalayas, Pakistan. *Tectonics* **1988**, *7*, 273–297. [[CrossRef](#)]
16. Critelli, S.; Garzanti, E. Provenance of the lower Tertiary Murree redbeds (Hazara-Kashmir Syntaxis, Pakistan) and initial rising of the Himalayas. *Sediment. Geol.* **1994**, *89*, 265–284. [[CrossRef](#)]
17. Javed, A.; Wahid, A.; Mughal, M.S.; Khan, M.S.; Qammar, R.S.; Ali, S.H.; Siddiqui, N.A.; Iqbal, M.A. Geological and petrographic investigations of the Miocene Molasse deposits in Sub-Himalayas, District Sudhnati, Pakistan. *Arab. J. Geosci.* **2021**, *14*, 1–24. [[CrossRef](#)]

18. Iqbal, O.; Baig, M.S.; Pervez, S.; Siddiqi, M.I. Structure and stratigraphy of Rumbli and Panjar areas of Kashmir and Pakistan with the aid of GIS. *J. Geol. Soc. India* **2018**, *91*, 57–66. [[CrossRef](#)]
19. Abbasi, N.; Khan, M.S. Sedimentary facies analysis of Nagri formation, Kashmir basin, sub-Himalayas, Pakistan. *Pak. J. Geol.* **2017**, *1*, 3–6. [[CrossRef](#)]
20. Zaheer, M.; Khan, M.S.; Mughal, M.S.; Abbasi, N. Petrography, provenance, diagenesis and depositional environment of Murree formation in Jhelum Valley, Sub Himalayas, Azad Jammu and Kashmir, Pakistan. *Arab. J. Geosci.* **2017**, *10*, 1–22. [[CrossRef](#)]
21. Abbasi, I.A. Fluvial Architecture And Depositional System Of The Miocene Molasse Sediments, Shakardara Formation, Southern Kohat, Pakistan. *J. Himal. Earth Sci.* **1994**, *27*, 81–98.
22. Zaleha, M.J. Intra-and extrabasinal controls on fluvial deposition in the Miocene Indo-Gangetic foreland basin, northern Pakistan. *Sedimentology* **1997**, *44*, 369–390. [[CrossRef](#)]
23. Mustafa, S.; Khan, M.A.; Khan, M.R.; Sousa, L.M.; Hameed, F.; Mughal, M.S.; Niaz, A. Building stone evaluation—A case study of the sub-Himalayas, Muzaffarabad region, Azad Kashmir, Pakistan. *Eng. Geol.* **2016**, *209*, 56–69. [[CrossRef](#)]
24. Aadil, N. Stratigraphy and structure of Sarda, Manil, Changpur and Naghal areas, district Kotli, Jammu & Kashmir. *J. Geol. Soc. India* **2013**, *82*, 639–648.
25. Khan, M.R.; Hameed, F.; Mughal, M.S.; Basharat, M.; Mustafa, S. Tectonic study of the Sub-Himalayas based on geophysical data in Azad Jammu and Kashmir and northern Pakistan. *J. Earth Sci.* **2016**, *27*, 981–988. [[CrossRef](#)]
26. Singh, B. Evolution of the Paleogene succession of the western Himalayan foreland basin. *Geosci. Front.* **2013**, *4*, 199–212. [[CrossRef](#)]
27. Ghosh, S.; Kumar, R. Petrography of Neogene Siwalik sandstone of the Himalayan foreland basin, Garhwal Himalaya: Implications for source-area tectonics and climate. *J. Geol. Soc. India* **2000**, *55*, 1–15.
28. Sanyal, P.; Bhattacharya, S.; Kumar, R.; Ghosh, S.; Sangode, S. Mio–Pliocene monsoonal record from Himalayan foreland basin (Indian Siwalik) and its relation to vegetational change. *Palaeogeogr. Palaeoclimatol. Palaeoecol.* **2004**, *205*, 23–41. [[CrossRef](#)]
29. Kundu, A.; Matin, A.; Mukul, M. Depositional environment and provenance of Middle Siwalik sediments in Tista valley, Darjiling District, Eastern Himalaya, India. *J. Earth Syst. Sci.* **2012**, *121*, 73–89. [[CrossRef](#)]
30. Debnath, A.; Taral, S.; Mullick, S.; Chakraborty, T. The Neogene Siwalik succession of the Arunachal Himalaya: A revised lithostratigraphic classification and its implications for the regional paleogeography. *J. Geol. Soc. India* **2021**, *97*, 339–350. [[CrossRef](#)]
31. Sigdel, A.; Sakai, T. Petrography of Miocene Siwalik Group sandstones, Karnali River section, Nepal Himalaya: Implications for source lithology and tectonic setting. *J. Nepal Geol. Soc.* **2013**, *46*, 95–110. [[CrossRef](#)]
32. Syangbo, D.K.; Tamrakar, N.K. Lithofacies and depositional environment of the Siwalik group in Samari-Sukaura river area, central Nepal. *Bull. Dep. Geol.* **2013**, *16*, 53–64. [[CrossRef](#)]
33. Rai, L.K.; Yoshida, K.; Kuritani, T. Reconstruction of the exhumation history of the eastern Nepal Himalaya based on provenance changes. *Sediment. Geol.* **2021**, *420*, 105920. [[CrossRef](#)]
34. Khan, M.A. Petrotectonic Framework Of The Siwalik Group Of Shingar Range With Special Reference To Its Petrography. *J. Himal. Earth Sci.* **1997**, *30*, 165–182.
35. Chaudhry, M.N.; Ashraf, M. Petrology of middle Siwalik rocks of Kotli area, Azad Kashmir. *J. Himal. Earth Sci.* **1981**, *14*, 183–191.
36. Ullah, K.; Arif, M.; Shah, M.T.; Abbasi, I.A. The Lower and Middle Siwaliks fluvial depositional system of the western Himalayan foreland basin, Kohat, Pakistan. *J. Himal. Earth Sci.* **2009**, *42*, 61–85.
37. Ullah, K.; Arif, M.; Shah, M.T. Petrography of sandstones from the Kamli and Chinji formations, southwestern Kohat plateau, NW Pakistan: Implications for source lithology and paleoclimate. *J. Himal. Earth Sci.* **2006**, *39*, 1–13.
38. Kundu, A.; Matin, A.; Eriksson, P.G. Petrography and geochemistry of the Middle Siwalik sandstones (tertiary) in understanding the provenance of sub-Himalayan sediments in the Lish River Valley, West Bengal, India. *Arab. J. Geosci.* **2016**, *9*, 1–18. [[CrossRef](#)]
39. Chutia, A.; Taye, C.D.; Daimari, J.; Chutia, D. Petrography and Clay Mineralogical Study of the Siwalik Group of Rocks Exposed along Pasighat-Mariyang Road Section, East Siang District, Arunachal Pradesh, Northeast India. *J. Geol. Soc. India* **2020**, *95*, 263–272. [[CrossRef](#)]
40. Mughal, M.S.; Khan, M.S.; Khan, M.R.; Mustafa, S.; Hameed, F.; Basharat, M.; Niaz, A. Petrology and geochemistry of Jura granite and granite gneiss in the Neelum Valley, Lesser Himalayas (Kashmir, Pakistan). *Arab. J. Geosci.* **2016**, *9*, 1–12. [[CrossRef](#)]
41. Marouer, D.; Chawla, H.; Challandes, N. Pre-alpine high-grade metamorphism in High Himalaya crystalline sequences: Evidence from Lower palaeozoic Kinnauer Kailas granite and surrounding rocks in the Sutlej Valley (Himachal Pradesh, India). *Ecolgeol. Helv.* **2000**, *93*, 207–220.
42. Gazzi, P. Le arenarie del flysch sopracretaceo dell'Appennino modenese; Correlazioni con flysch di Monghidoro. *Min. Petrogr. Acta* **1966**, *12*, 69–97.
43. Goldsmith, J.R.; Graf, D.L. Structural and compositional variations in some natural dolomites. *J. Geol.* **1958**, *66*, 678–693. [[CrossRef](#)]
44. Goldsmith, J.R.; Heard, H.C. Subsolidus phase relations in the system CaCO₃-MgCO₃. *J. Geol.* **1961**, *69*, 45–74. [[CrossRef](#)]
45. Miall, A. Sedimentary facies, basin analysis, and petroleum geology. *Geol. Fluv. Depos.* **1996**, *2*, 582.
46. Miall, A.D. Architectural-element analysis: A new method of facies analysis applied to fluvial deposits. *Earth-Sci. Rev.* **1985**, *22*, 261–308. [[CrossRef](#)]
47. Ulak, P.D. Lithostratigraphy and late Cenozoic fluvial styles of Siwalik group along Kankai River section, East Nepal Himalaya. *Bull. Dep. Geol.* **2009**, *12*, 63–74. [[CrossRef](#)]

48. Rai, L.K.; Yoshida, K. Sedimentary facies analysis of the fluvial environment in the Siwalik Group of eastern Nepal: Deciphering its relation to contemporary Himalayan tectonics, climate and sea-level change. *Prog. Earth Planet. Sci.* **2021**, *8*, 1–18. [[CrossRef](#)]
49. Skelly, R.L.; Bristow, C.S.; Ethridge, F.G. Architecture of channel-belt deposits in an aggrading shallow sandbed braided river: The lower Niobrara River, northeast Nebraska. *Sediment. Geol.* **2003**, *158*, 249–270. [[CrossRef](#)]
50. Folk, R.L. Practical petrographic classification of limestones. *AAPG Bull.* **1959**, *43*, 1–38.
51. Dickinson, W.R.; Beard, L.S.; Brakenridge, G.R.; Erjavec, J.L.; Ferguson, R.C.; Inman, K.F.; Knepp, R.A.; Lindberg, F.A.; Ryberg, P.T. Provenance of North American Phanerozoic sandstones in relation to tectonic setting. *Geol. Soc. Am. Bull.* **1983**, *94*, 222–235. [[CrossRef](#)]
52. Ingersoll, R.V.; Suczek, C.A. Petrology and provenance of Neogene sand from Nicobar and Bengal fans, DSDP sites 211 and 218. *J. Sediment. Res.* **1979**, *49*, 1217–1228.
53. Basu, A.; Young, S.W.; Suttner, L.J.; James, W.C.; Mack, G.H. Re-evaluation of the use of undulatory extinction and polycrystallinity in detrital quartz for provenance interpretation. *J. Sediment. Res.* **1975**, *45*, 873–882.
54. Grantham, J.H.; Velbel, M.A. The influence of climate and topography on rock-fragment abundance in modern fluvial sands of the southern Blue Ridge Mountains, North Carolina. *J. Sediment. Res.* **1988**, *58*, 219–227. [[CrossRef](#)]
55. Weltje, G.J. *Provenance and Dispersal of Sand-Sized Sediments: Reconstruction of Dispersal Patterns and Sources of Sand-Sized Sediments by Means of Inverse Modelling Techniques*; Utrecht University: Utrecht, The Netherlands, 1994; Volume 121.
56. Suttner, L.J.; Dutta, P.K. Alluvial sandstone composition and paleoclimate; I, Framework mineralogy. *J. Sediment. Res.* **1986**, *56*, 329–345.
57. Kumari, N.; Mohan, C. Basics of clay minerals and their characteristic properties. *Clay Clay Min.* **2021**, *24*, 1–29.
58. Lu, T.; Xia, T.; Qi, Y.; Zhang, C.; Chen, W. Effects of clay minerals on transport of graphene oxide in saturated porous media. *Environ. Toxicol. Chem.* **2017**, *36*, 655–660. [[CrossRef](#)]
59. Miall, A.D. Facies models. In *Stratigraphy: A Modern Synthesis*; Springer: Berlin/Heidelberg, Germany, 2016; pp. 161–214.
60. Yuan, D.Y.; Ge, W.P.; Chen, Z.W.; Li, C.Y.; Wang, Z.C.; Zhang, H.P.; Zhang, P.Z.; Zheng, D.W.; Zheng, W.J.; Craddock, W.H. The growth of northeastern Tibet and its relevance to large-scale continental geodynamics: A review of recent studies. *Tectonics* **2013**, *32*, 1358–1370. [[CrossRef](#)]
61. Ghazi, S.; Mountney, N.P. Facies and architectural element analysis of a meandering fluvial succession: The Permian Warchha Sandstone, Salt Range, Pakistan. *Sediment. Geol.* **2009**, *221*, 99–126. [[CrossRef](#)]
62. Meigs, A.J.; Burbank, D.W.; Beck, R.A. Middle-late Miocene (>10 Ma) formation of the Main Boundary thrust in the western Himalaya. *Geology* **1995**, *23*, 423–426. [[CrossRef](#)]
63. Garzanti, E.; Critelli, S.; Ingersoll, R.V. Paleogeographic and paleotectonic evolution of the Himalayan Range as reflected by detrital modes of Tertiary sandstones and modern sands (Indus transect, India and Pakistan). *Geol. Soc. Am. Bull.* **1996**, *108*, 631–642. [[CrossRef](#)]
64. Joshi, M.; Tiwari, A. Quartz C-axes and metastable phases in the metamorphic rocks of Almora Nappe: Evidence of pre-Himalayan signatures. *Curr. Sci. Bangalore* **2004**, *87*, 995–998.
65. Gao, C.; Ji, Y.; Wu, C.; Jin, J.; Ren, Y.; Yang, Z.; Liu, D.; Huan, Z.; Duan, X.; Zhou, Y. Facies and depositional model of alluvial fan dominated by episodic flood events in arid conditions: An example from the Quaternary Poplar Fan, north-western China. *Sedimentology* **2020**, *67*, 1750–1796. [[CrossRef](#)]
66. Drake, A.A., Jr.; Sinha, A.; Laird, J.; Guy, R. The taconic orogen. In *The Appalachian-Ouachita Orogen in the United States, The Geology of North America*; Geological Society of America: Boulder, CO, USA, 1989; Volume 2, pp. 101–177.
67. Crowley, J.L.; Myers, J.S.; Sylvester, P.J.; Cox, R.A. Detrital zircon from the Jack Hills and Mount Narryer, Western Australia: Evidence for diverse > 4.0 Ga source rocks. *J. Geol.* **2005**, *113*, 239–263. [[CrossRef](#)]
68. Adhikari, S.K.; Sakai, T. Petrography of the Neogene Siwalik Group sandstones, Khutia Khola section, Nepal Himalaya: Implications for provenance, paleoclimate and tectonic setting. *J. Nepal Geol. Soc.* **2017**, *53*, 17–30. [[CrossRef](#)]
69. Goudie, A.S. Global warming and fluvial geomorphology. *Geomorphology* **2006**, *79*, 384–394. [[CrossRef](#)]